Design of Phosphate Ion Sensors and an All-Solid pH Sensor and Construction of an Automatic Nutrient Solution Management System for Hydroponics

Xu Kebin

2020

Table of contents

General introduction

The hydroponic culture is hard to be affected by blight and disease-causing germs, and it is regarded as a core technology of the plant factory to supply grains and vegetables steadily regardless of the climatic condition. In order to grow agricultural products effectively, temperature, humidity, irradiation light (wavelength, intensity, period) and nutrient concentrations have been tried to optimized up to now. The proper nutrient control of the culture fluid is especially important to improve the yield. It is necessary for the continuous nutrient control to measure continuously the nutrient concentration. Since the culture fluid can be used for the measurement of nutrient concentrations without any pretreatment, the electrochemical measurement using the ion-selective electrodes (ISEs) is very attractive. However, the ISEs except the K^+-ISE are not suitable for the long-term monitoring due to the stability and reproducibility. In particular, the $H_2PO_4^-$-ISE and HPO_4^{2-}-ISE are not commercially available. Although there have been several reports on the $H_2PO_4^-$-ISE and HPO_4^{2-}-ISE (Pi-ISE), it is known that they are not stable. Then, the ISE of NO_3^- which can be used for a long term measurement and which was constructed by the author's group was used for the monitoring system of nutrient concentrations.

Three major nutrients of the plant are nitrogen, potassium and phosphorus. As for phosphorus, phosphorus exists as a phosphate ion (Pi) in the natural world. The concentration of phosphate ion is usually measured by spectroscopic analysis or chromatography. However, the pretreatment such as the filtration is required for these methods. In addition, we cannot measure the concentration of Pi directly and in situ by these methods. Using the Pi-ISE, it is easy to monitor the concentration of Pi directly and in situ. In the present study, we constructed stable Pi-ISEs by optimization of material composition. Therefore we made the ion-selective electrodes of the phosphate ions ($H_2PO_4^-$, HPO_4^{2-}).

The pH measurement is required in the various fields such as chemical industry, food industry, environment science, medical science and basic science. The pH value is usually determined using a pH indicator and a glass electrode. Because the glass electrode is particularly easy to use and stable, the glass electrode is used widely. However, the glass electrode is easily broken and it is difficult to miniaturize. On the other hand, it is well known that platinum group metal such as Pt, Pd, etc. can be used as a base material of the standard hydrogen electrode. Since Pd is one of hydrogen storage metals, H_2 is spontaneously released from the Pd electrode which sufficiently stores hydrogen. In order to overcome the problems of the glass electrode (fragility and processing property), we made a new pH sensor using Pd electrode.

Chapter1

Phosphate Ion Sensor Using a Cobalt Phosphate Coated Cobalt Electrode

Phosphorous is one of three major nutritional elements for plants and usually exists as phosphate ions in nature. For hydroponic culturing and wastewater treatment, the development of a high-performance phosphate sensor would be very helpful. A novel phosphate ion-selective electrode was constructed using a cobalt phosphate surface coated cobalt electrode. The potential response seems to be caused by the formation of $Co(H_2PO_4)_2$ in the coexistence of CoO and $Co(OH)_2$. The sensor exhibited a linear response to $H_2PO_4^-$ in the concentration range from 1.0×10^{-5} to 1.0×10^{-1} mol L^{-1} at a pH range from 4.0 to 6.5 with a slope of −39 mV dec^{-1}. The sensor was unaffected by common anions, such as chloride, carbonate, and sulfate. The electrode maintained stability for at least 4 weeks in a live hydroponics system when sufficient $Co_3(PO_4)_2 \cdot 8H_2O$ was deposited on the Co electrode.

Introduction

Phosphate ion analysis has become a hot topic in recent decades for advanced hydroponic culturing and environmental wastewater treatment [1,2]. The concentration of phosphate ion is usually determined using high-performance liquid chromatography or spectroscopic methods using the molybdenum blue reaction, complex formation of molybdophosphate with basic dye compounds, and indirect determination with lanthanum chloranilate after a sample pretreatment, such as filtration and solution preparation [3-6]. Thus, it is difficult to continuously monitor the concentration of phosphate ions. In recent decades, electrochemical measurements using ion-selective electrodes (ISE) have been developed. ISE allow for simple, fast, stable, low cost, and portable analysis of target analytes [7-17]. For phosphate ISEs, various approaches have been attempted: 1) metal|metal compound coupling electrodes [7-12]; 2) solid membrane electrodes [13]; 3) heterogeneous metal membrane electrodes [14]; and 4) polyvinylchloride (PVC) membrane electrodes impregnated with organic solutions [15-17]. In particular, cobalt has often been utilized as a base material for the phosphate sensor [2, 12, 18–25]. Xiao *et al.* reported that the cobalt electrode, the surface of which was coated by a cobalt oxide (CoO) layer, showed a selective potentiometric response to $H_2PO_4^-$ and the reporting mechanism of the CoO-modified electrode was discussed based on the host-guest chemistry of a nonstoichiometric cobalt oxide compound [7]. Meruva and Meyerhoff proposed a mixed potential mechanism based off the behavior of the Co electrode in the presence of phosphate and oxide species [18]. Although many studies exist on the types of phosphate-sensing Co electrodes, including a microelectrode type [19–21], a cobalt film type [22,23], a screen printing type [24], and a flow injection type [2,25], the proposed mechanism by Meruva and Meyerhoff appears to be universally applicable. On the other hand, Kidosaki *et al.* suggested a different

response mechanism [26]. They believed that the reporter compound was $Co(H_2PO_4)_2$ and that the reaction was coupled with the reduction of oxygen. Since it is well known that the potential of the Co-modified electrode is not stable, the details of the reporting mechanism are still unclear [8,10]. In addition, the influence of pH in the monitoring system on the stability of the Co-modified electrode has been reported [19]. In the present study, an ISE for the dihydrogenphosphate ion ($H_2PO_4^-$) was constructed by electrodepositing cobalt phosphate hydrate ($Co_3(PO_4)_2 \cdot 8H_2O$) onto the surface of the Co electrode. The electrochemical characteristics were then evaluated and the $H_2PO_4^-$ reporting mechanism was investigated by considering a mixed potential system.

Experimental

Reagents

All chemical reagents were of analytical grade and were used without further purification. Co wire （φ1 mm, 99.99%）was purchased from the Nilaco Co., Ltd. Sodium dihydrogenphosphate dihydrate (NaH_2PO_4), sodium hydrogenphosphate monohydrate (Na_2HPO_4), potassium nitrate (KNO_3), sodium chloride (NaCl), sodium sulfate (Na_2SO_4), sodium acetate (CH_3COONa), sodium hydrogencarbonate ($NaHCO_3$) and sodium hydroxide (NaOH) were purchased from Wako. Co. Ltd. Hydrochloric acid (HCl) was obtained from Kishida Co. Ltd.

Apparatus

Electrochemical measurements were conducted using electrometers HE-106A (Hokuto Denko Co., Ltd.), a potentiostat/galvanostat HA1010mM1A (Hokuto Denko Co., Ltd.), a function generator HB305 (Hokuto Denko Co., Ltd.) and an A/D converter (GL900, Graphtec. Co., Ltd. The electrode surface before and after the electrolysis was observed by a scanning electron microscopy VHX-D500 (Keyence Co., Ltd.). By use of pH meter PH-230SD (Lutron Co., Ltd. Taiwan), the pH of the solution was prepared and measured. The concentration of dissolved oxygen, DO, in the aqueous solution was measured by an oxygen electrode E101 (Optoscience Co., Ltd.). According to the methods of Lee et al. [19], argon, air and oxygen were bubbled for several minutes until the current of an oxygen sensor was kept at a constant value in order to prepare 0%, 21% and 100% DO solutions. The saturated concentration of O_2 in water (at 20°C) is estimated at about 8.75 mg L^{-1}, and the potentiometric response is similar to that in the case of about 21%. Here, the concentration of oxygen in the test solution was monitored with a commercial oxygen electrode. The chemical composition of the electrodeposits was examined by an XRD meter SmartLab (Rigaku Corp.).

Preparation of Co modified electrodes

At first, the surface of the cobalt wire (diameter: □1 mm, length: 100 mm) was polished by

sandpapers of #80, #240 and #1000, respectively. It was then washed for 30 min by an ultrasonic cleaner. The cobalt wire was covered with a silicone tube except both ends of the electrode, and one end of the silicone tube was coated with epoxy resin to avoid the penetration of the solution into the gap between the cobalt electrode and the silicone tube. Thus one end of the cobalt wire of which length was 10 mm was used as a working electrode. The electrode was used for the measurement of cyclic voltammogrms.

In order to coat the electrode surface with the cobalt phosphate, the constant potential (–0.3 V *vs.* Ag|AgCl|sat. KCl) was applied for about 2 hours until the anodic current decreased to about 0 A, as shown in the inset of Fig. 2. After the surface of the Co electrode was washed with double distilled water, the modified electrode was dried and was stored in Argon gas atmosphere.

Electrochemical measurement

All potentiometric measurements were carried out with a two-electrode system using a saturated Ag|AgCl reference electrode and phosphate-sensing electrodes (3 sets as parallel), and both a temperature and an oxygen sensors were used simultaneously. In the present study, the ISE potential was measured under constant DO concentrations (about 8.75 mg L^{-1}) by bubbling air through the system except when DO concentration was changed.

Results and Discussion

Cyclic voltammograms of Co electrode in phosphate ion system

Cyclic voltammograms were obtained using the Co electrode in aqueous solutions in the presence and absence of NaH_2PO_4 at pH 7, as shown in Fig.1.

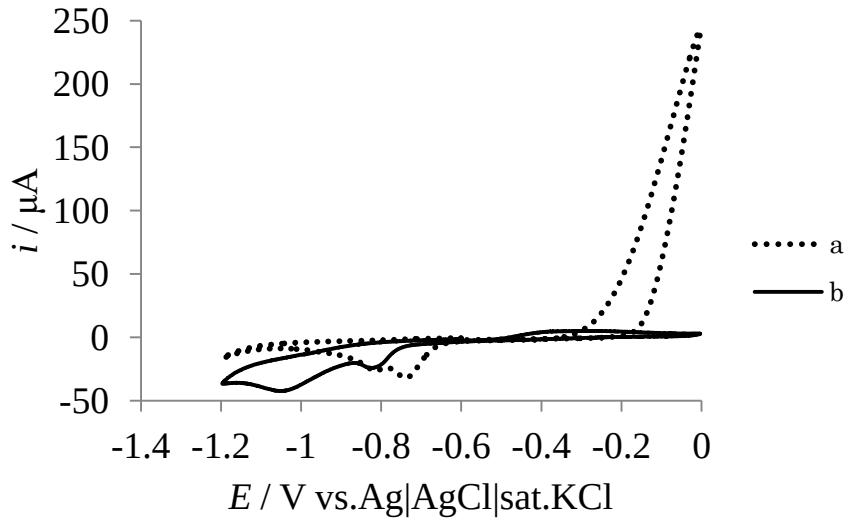

Fig. 1 Cyclic voltammograms of the cobalt electrode in 0.1 M NaCl (a) and 0.1 M NaH_2PO_4 (b) at pH 7. Potential scanning rate: 50 mV s^{-1}. Electrode area: 0.785 mm^2.

The potential was scanned for four cycles in the range from −1.2 V to 0 V (vs. Ag|AgCl|sat.KCl)) at a scan rate of 50 mV s^{-1}. In the absence of $H_2PO_4^-$, the anodic current started to flow at −0.35 V and two cathodic peaks appeared at −0.74 V and −0.82 V, respectively, in the negative potential scan. Based on the Pourbaix diagram in Fig.2, the standard potential of the $Co|Co^{2+}$ couple is around −0.48 V [27]. Thus, the two cathodic peaks can be assigned to the reduction of Co^{2+} to Co, caused by the reduction of $Co(OH)_2$ and/or Co oxides (CoO and/or Co_2O_3), respectively. By considering the pH value of the experiment, the reduction of $Co(OH)_2$ was more probable than that of Co oxides. In the presence of $H_2PO_4^-$ under aqueous conditions (curve **b**), another anodic peak appeared around −0.3 V, and the anodic wave that existed at the more positive potential (like the final rise) in the absence of H_2PO_4 disappeared. The anodic peak seems to appear due to the formation of cobalt phosphate since the anodic peak height was $H_2PO_4^-$ concentration dependent, as expressed from Fig. 3. In this case, the following reactions are believed to occur on the surface of the Co electrode in this potential region.

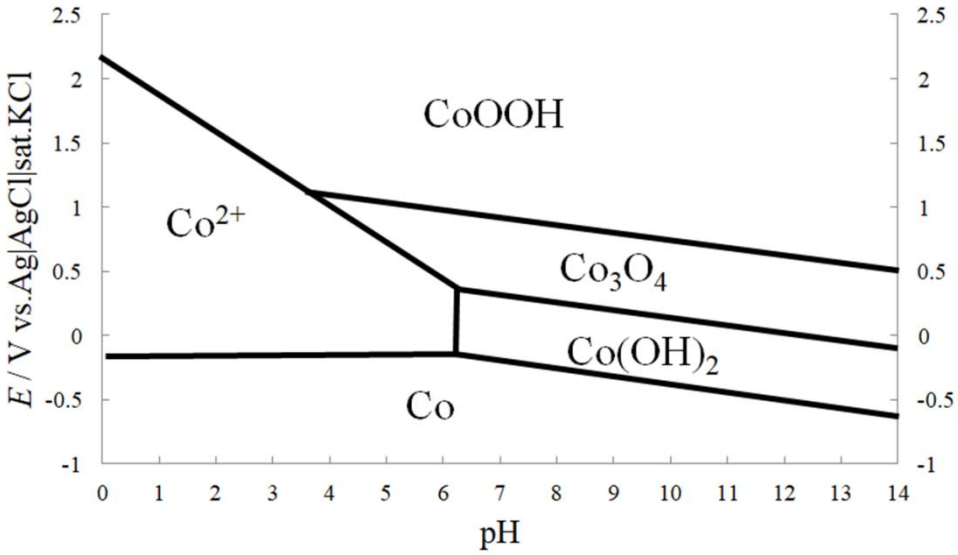

Fig. 2 Pourbaix diagram of the Co-H_2O system at 25 °C [22].

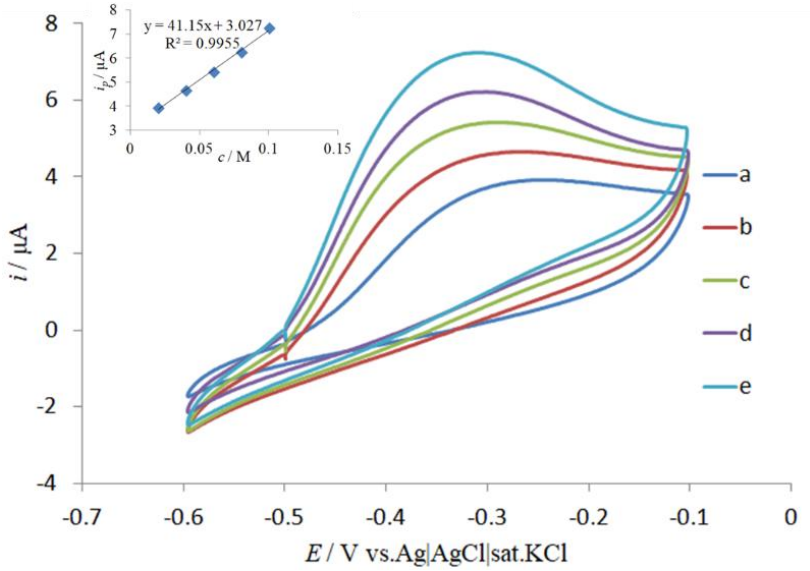

Fig. 3 Cyclic voltammograms in the presence of $H_2PO_4^-$ at pH 7.0: (a) 0.02 M, (b) 0.04 M, (c) 0.06 M, (d) 0.08 M, and (e) 0.10 M.
Potential scanning rate: 50 mV s^{-1}. Electrode area: 0.785 mm^2.
Inset: Concentration dependence of the cathodic peak current (I_p)
Potential scanning rate: 50 mV s^{-1}. Electrode area: 0.785 mm^2.

$$Co^{2+} + 2e^- \rightleftharpoons Co \quad (1\text{-}1)$$

$$Co(OH)_2 + 2e^- \rightleftharpoons Co + 2OH^- \quad (1\text{-}2)$$

$$Co(H_2PO_4)_2 + 2e^- \rightleftharpoons Co + 2H_2PO_4^- \quad (1\text{-}3)$$

In addition, the anodic current peak height greatly decreased when the pH approached the pK_{a2} value (7.2) of phosphate and the potential scanning rate increased, as expressed in Fig. 4 and Fig. 5. Taking into account these characteristics, that $Co(H_2PO_4)_2$ is the response active material to $H_2PO_4^-$ under aqueous conditions is predictable [28]. Accordingly, the Co electrode coated by cobalt phosphate on the surface was fabricated as a $H_2PO_4^-$-ISE electrode. The anodic current, due to the oxidation of Co, which appears above −0.35 V was inhibited by the cobalt phosphate layer.

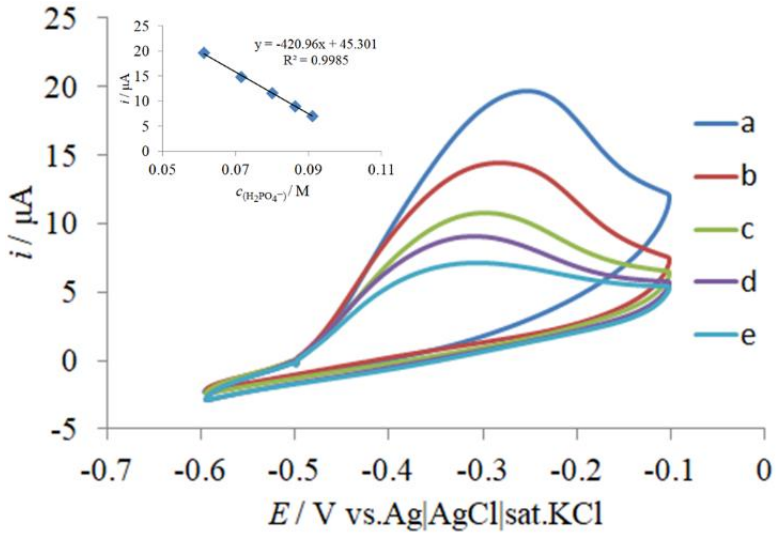

Fig. 4 Cyclic voltammograms in the presence of 0.1 M NaH2PO4 at various DO concentration: (a) pH 6.2, (b) pH 6.4, (c) pH 6.6, (d) pH 6.8, and (e) pH 7.0.
Potential scanning rate: 50 mV s^{-1}. Electrode area: 0.785 mm^2.
Inset: $H_2PO_4^-$ concentration dependence of the cathodic peak current (Ip) Potential scanning rate: 50 mV s^{-1}. Electrode area: 0.785 mm^2.

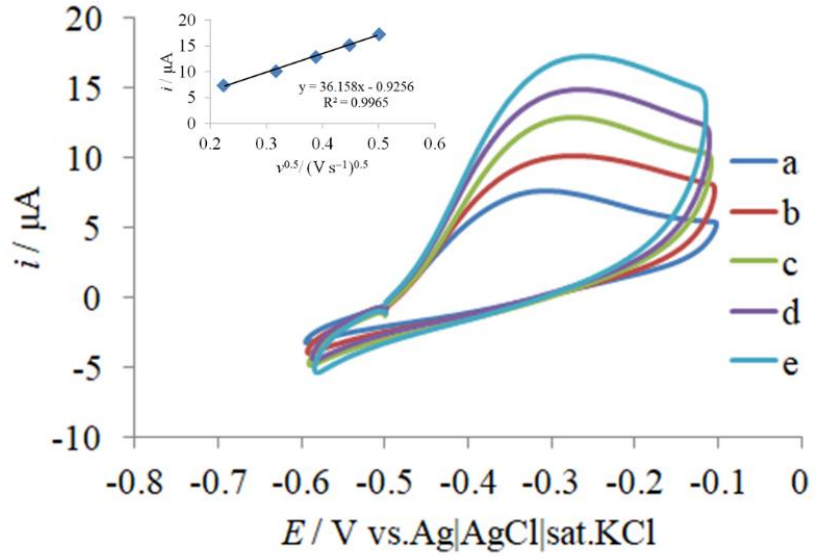

Fig. 5 Cyclic voltammograms in the presence of 0.1 M NaH2PO4 at pH 7.0 at various scanning rates: (a) 50 mV s–1, (b) 100 mV s–1, (c) 150 mV s–1, (d) 200 mV s–1, and (e) 250 mV s–1.
Potential scanning rate: 50 mV s^{-1}. Electrode area: 0.785 mm^2.

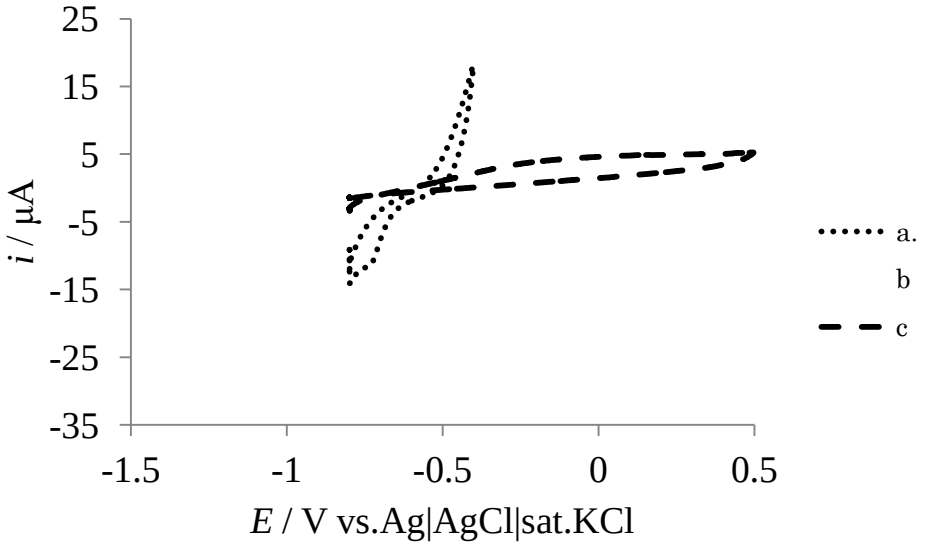

Fig. 6 Cyclic voltammograms of the cobalt electrode in 0.1 M NaH_2PO_4 at different pH: (a) pH 5, (b) pH 7, and (c) pH 9.
Potential scanning rate: 50 mV s^{-1}. Electrode area: 0.785 mm^2.
Inset: Time-course of the current under a constant potential of −0.3 V. Electrode area: 0.785 mm^2.

There are two cathodic peaks in curve **b** of Fig. 1. The peak appearing near −0.82 V is the same cathodic peak observed in the absence of $H_2PO_4^-$ (curve **a** of Fig. 1), and the cathodic wave is thought to result from the reduction of $Co(OH)_2$ (and/or CoO) to Co. The other peak appearing near −1.04 V was attributed to the reduction of $Co(H_2PO_4)_2$ to Co.

Fig. 6 presents the cyclic voltammograms of the Co electrode in 0.1 M (mol dm^{-3}) phosphate ion at several pH values. At pH 5, the anodic current due to the oxidation of Co to Co^{2+} was observed at a potential more positive than −0.65 V and a cathodic wave, which might be caused by the reduction of Co^{2+} or $Co(H_2PO_4)_2$ to Co, was observed at a more negative potential than −0.7 V. At pH 7, the anodic peak appearing near −0.3 V was caused by the formation of $Co(H_2PO_4)_2$. At pH 9, the anodic current gradually flowed above −0.6 V, but the magnitude was smaller than that at pH 7. In addition, the cathodic reaction was also inhibited. These performance losses were likely caused by the formation of a $Co(OH)_2$ layer at the electrode surface. According to the Pourbaix diagram of the Co-H_2O system (Fig. 2) [29], reaction (1) mainly occurs in acidic conditions. Since $H_2PO_4^-$ is the main form of phosphate in a pH 2.1 to 7.2 solution, it is possible for reaction (3) to proceed in a pH 5.0 solution. At pH 7.0, both reaction (2) and (3) can occur. Since the monohydrogenphosphate ion is the main form of phosphate at pH 9, it is thought that the anodic current of reaction (3) was very low and that reaction (2) was dominant. Based on the characteristics of the Co electrode, the electrodeposit was estimated to be $Co(H_2PO_4)_2$.

In order to verify that dihydrogen phosphate ion was the responding ion, cyclic votammograms on the cobalt electrode in the presence of the same concentration of total phosphate ion at different pH were measured as shown in Fig. 4. Based on the diagram of the distribution of phosphate species (Inset of Fig. 4), we can estimate the concentration ratio of $H_2PO_4^-$ to HPO_4^{2-} in the pH region from 6.2 to 7.0 based on the following relations [27];

$$H_3PO_4 + H_2O \rightleftharpoons H_2PO_4^- + H_3O^+ \quad (1\text{-}4)$$

$$H_2PO_4^- + H_2O \rightleftharpoons HPO_4^{2-} + H_3O^+ \quad (1\text{-}5)$$

$$HPO_4^{2-} + H_2O \rightleftharpoons PO_4^{3-} + H_3O^+ \quad (1\text{-}6)$$

$$K_{a1} = \frac{[H_2PO_4^-][H_3O^+]}{[H_3PO_4]} = 7.5\times10^{-3} \quad (1\text{-}7)$$

$$K_{a2} = \frac{[HPO_4^{2-}][H_3O^+]}{[H_2PO_4^-]} = 6.23\times10^{-8} \quad (1\text{-}8)$$

$$K_{a3} = \frac{[PO_4^{3-}][H_3O^+]}{[HPO_4^{2-}]} = 2.2\times10^{-13} \quad (1\text{-}9)$$

Electrodeposition of Co electrode

Since the anodic wave appearing between −0.6 and 0 V in Fig. 6 was related to the formation of $Co(H_2PO_4)_2$, −0.3 V was selected as the applied potential for electrodepositing the coating onto the surface of the Co electrode. As shown in the inset of in Fig. 6, the current varied when the constant potential (E= −0.3 V) was applied. The current did not exponentially decrease, and once it increased until about 1000s after the starting the electrolysis. The initial current increase could be caused by the increase in the electrode area. Then the current gradually decreased to about 0 A within 8000s. Product formation (cobalt phosphate complex) was considered to have been gradually inhibited by the solid product layer. After the electrolysis (total electric quantity was about 0.3 C), purple compounds were deposited onto the surface of the cobalt electrode. Fig.7A shows the images of a scanning electron microscope (SEM) at the surface of the bare cobalt electrode (before electrolysis). The surface of the cobalt electrode looked smooth and homogenous before the electrolysis. However, the SEM image of the electrode surface was coated with crystal electrodeposits after electrolysis, as shown in Fig. 7B.

(a) (b)

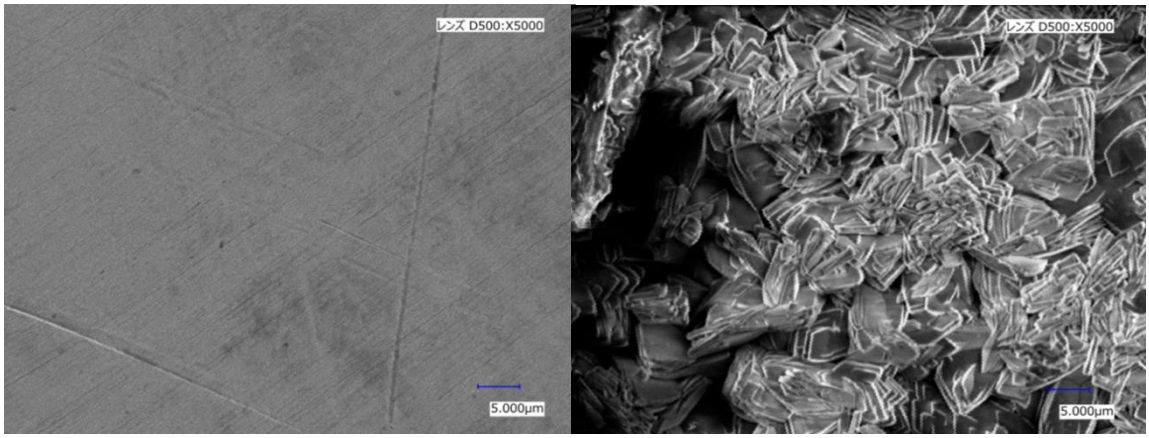

Fig. 7. SEM images of the bare cobalt electrode before electrolysis (a) and after electrolysis (b).

The crystallinity and composition of the electrodeposits was determined using X-ray diffraction analysis (XRD). Crystalline $Co_3(PO_4)_2$•$8H_2O$ was found, as shown in Fig. 8 [29]. The reactions between $Co_3(PO_4)_2$ and $Co(H_2PO_4)_2$ are believed to be as follows:

$$3Co_3(PO_4)_2 + 6H_2O + O_2 \rightleftharpoons 3Co(H_2PO_4)_2 + 2Co_3O_4 \quad (1\text{-}10)$$

$$Co_3(PO_4)_2 + 2H_2O \rightleftharpoons Co(H_2PO_4)_2 + 2CoO \quad (1\text{-}11)$$

$$3Co_3(PO_4)_2 + 4H_2O \rightleftharpoons 3Co(H_2PO_4)_2 + 2Co(OH)_2 \quad (1\text{-}12)$$

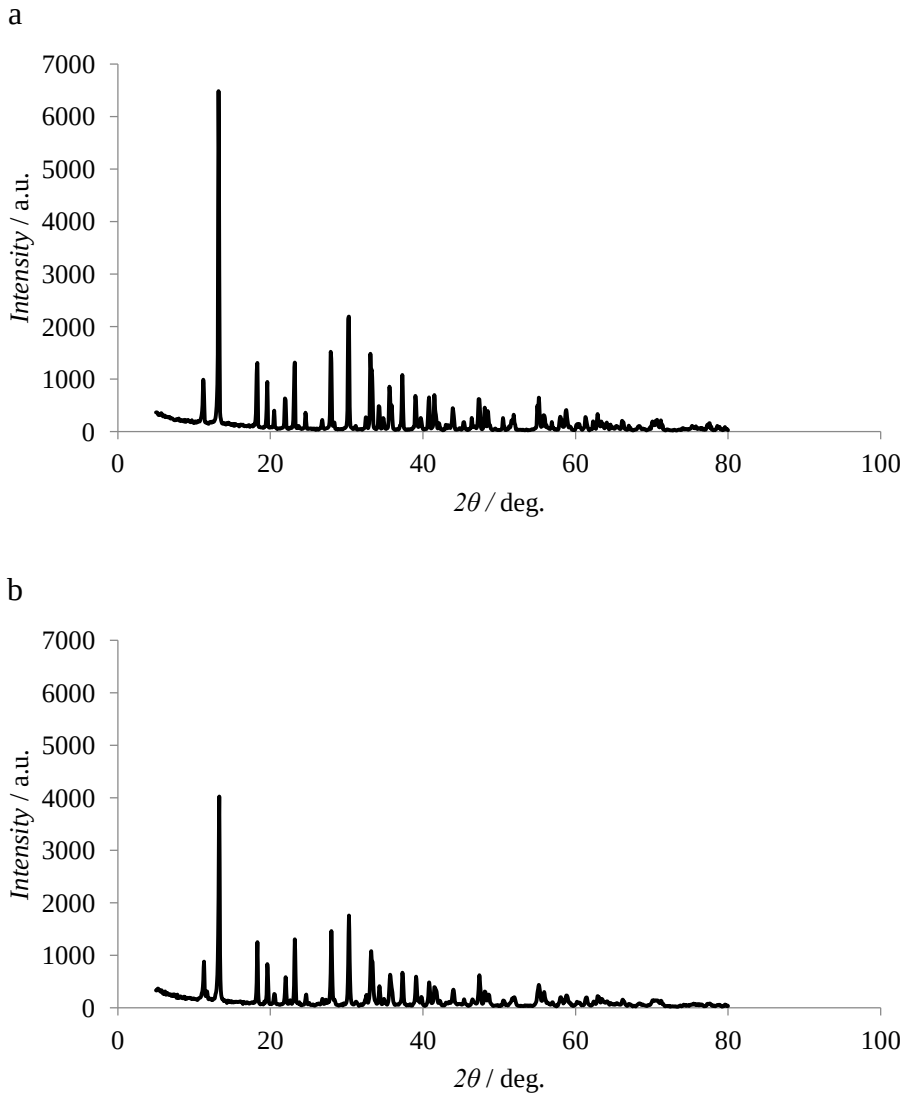

Fig. 8 XRD patterns of $Co_3(PO_4)_2 \cdot 8H_2O$ (a) and the electrodeposit (b).

Influence of dissolved oxygen

It is concluded that the potential of the $H_2PO_4^-$-ISE is a mixed potential because two or more electrochemical reactions occurred at the same time. In particular, it is thought that the redox reactions of Co (Co|Co^{2+}, Co|$Co(OH)_2$, Co|CoO, Co|Co_3O_4, *etc*) and the phosphorylation coexist in the potential region. Cyclic voltammograms obtained at a scan rate of 50 mV s^{-1} in 0.1 M $H_2PO_4^-$ at pH 7.0 are shown in Fig. 9. The curves were recorded at the different DO concentration (0, 21 and 100 %). The

anodic waves due to the oxidation of Co to Co^{2+} were observed at more positive potential than about −0.5 V. The inset of Fig. 9 indicates an illustration enlarged around −0.5 V. Thus, the zero-current potential depended on the DO concentration. It seems that the dependence of DO concentration affected

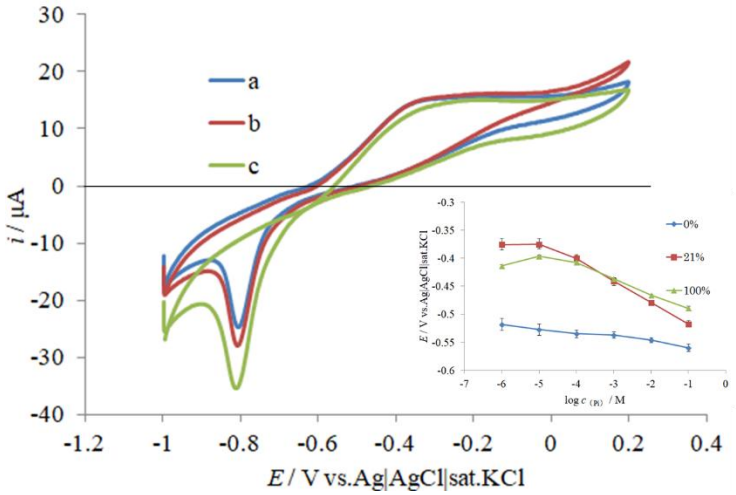

Fig. 9 Cyclic voltammograms in the presence of 0.1 M NaH_2PO_4 at pH 7.0 at various scanning rates: (a) 0 %, (b) 21 %, and (c) 100 %.
Potential scanning rate: 50 mV s^{-1}. Electrode area：0.785 mm^2.
Inset: Dependence of the cathodic peak current (I_p) versus scan rate.
Potential scanning rate: 50 mV s^{-1}. Electrode area：0.785 mm^2.

the phosphorylation. Comparing the case of the presence of phosphate ion, the zero-current potential shifted toward the opposite direction (positive potential) with an increase of DO concentration. This trend would be caused by the inhibition of the formation of the oxide layer on the phosphorylation.

On the other hand, the interference from dissolved oxygen (DO) is recognized, as shown in Fig. S5 [7, 19, 28]. The waveforms of the cyclic voltammograms appear correct, but the zero-current potential was affected by the DO concentration. The effect was evaluated at the DO concentrations of 0%, 21%, and 100%, the DO influence on the potentiometric response to phosphate ion is shown in the inset of Fig. 9. Thus, the resting potential is dependent on the DO concentration. Notably, the $H_2PO_4^-$-ISE is inactive at 0% DO. This provides supporting evidence that reaction (4) is involved between $Co_3(PO_4)_2$ and $Co(H_2PO_4)_2$. The above characteristics indicate that the electrode reaction around the zero-current potential is composed from multiple electrode reactions and that the resting potential is a mixed potential. Under similar DO concentrations, the resting potential of the modified Co electrode was stable and constant. In the hydroponic culture, the ISE potential was measured under the constant DO concentration (about 8.75 mg L^{-1}) by air bubbling.

Response characteristics to phosphate ion of Co electrode

Fig. 10 illustrates the dynamic response characteristics of the modified Co electrode to the concentration of $H_2PO_4^-$ at pH 4. In this case, the pH was adjusted using NaOH and HCl solutions. The modified Co electrode showed a linear response with a slope of −39±1 mV dec^{-1} to phosphate ion in the concentration range from 10^{-5} to 10^{-1} M.

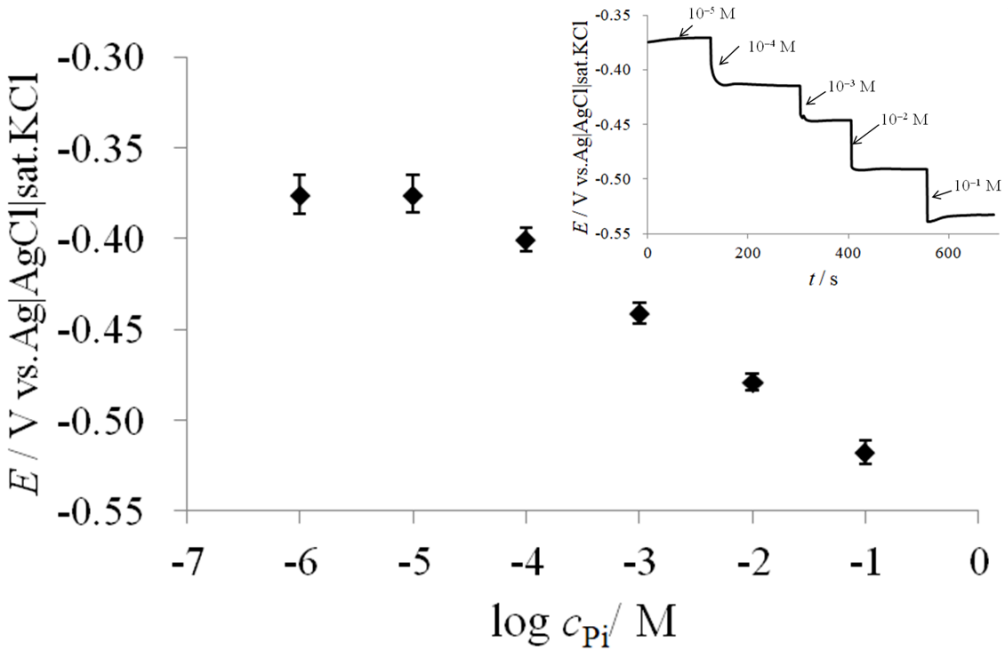

Fig. 10 Typical calibration curve of the phosphate sensor system at pH 4
Inset: The response time of the phosphate sensor system to the addition of phosphate ion.

The practical response time was recorded by changing the concentration of $H_2PO_4^-$ from 1.0 × 10^{-5} to 1.0 × 10^{-1} M, as shown in the inset of Fig. 10. The potential stabilized within 30 s after the addition of $H_2PO_4^-$ into the test cell. The fluctuation of the potential was within ±2 mV over 24 h, as indicated in Fig. 11. This indicates the potential response was stable and the ISE could be run continuously at least 4 weeks.

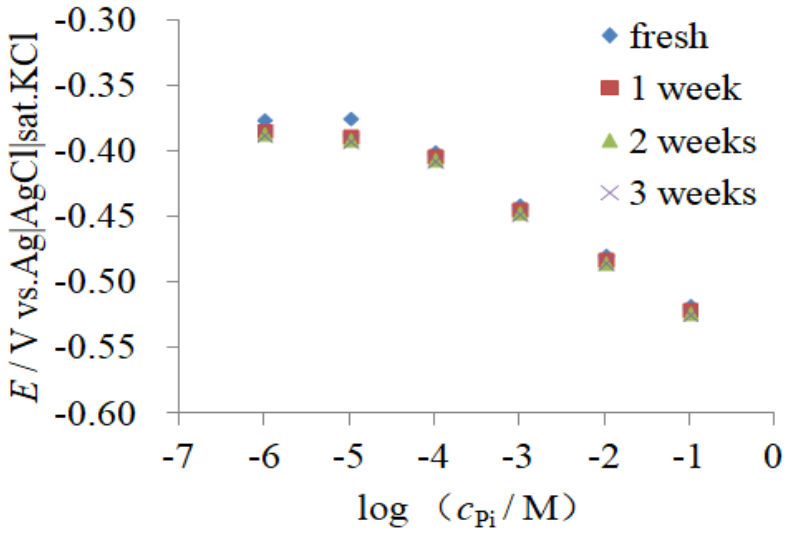

Fig. 11 Stability of current phosphate ion sensor

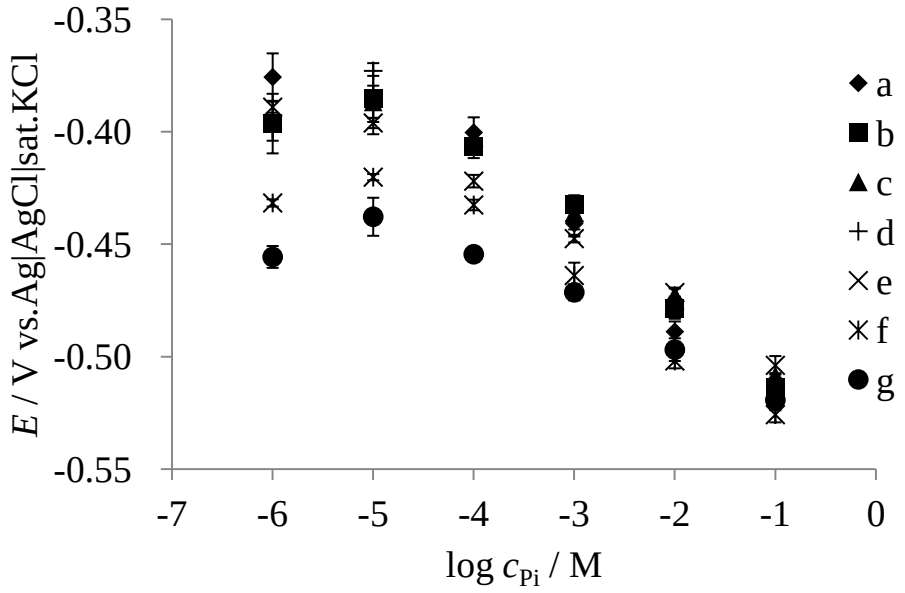

Fig. 12 Influence of pH on the potential response of the modified cobalt electrode: (a) pH 4.0, (b) pH 5.0, (c) pH 6.0, (d) pH 6.5, (e) pH 7.0, (f) pH 8.0, and (g) 9.0.

In the pH range from 4.0 to 6.5, the linear response property was unchanged, as shown in Fig. 12. At pH > 7.0, the slope decreased as pH increased. Additionally, the detection limit deteriorated. Since $Co(OH)_2$ is the dominant species under basic conditions, degradation of the modified electrode surface is possible. Chen *et al.* reported the negative influence on the electrode was caused by precipitation of $Co(OH)_2$ (K_{sp}: 1.6×10^{-15}) on the surface of the Co electrode [25].

The selectivity coefficients k_{ij}^{pot} of HCO_3^-, NO_3^-, CH_3COO^-, SO_4^{2-}, and Cl^- were evaluated using the mixed solution method. The k_{ij}^{pot} of HCO_3^-, NO_3^-, CH_3COO^-, SO_4^{2-}, and Cl^- were −2.1, −2.5, −3.2, −4.0, and −4.0, respectively.

Conclusion

In conclusion, a novel phosphate ion-selective electrode was developed by coating a Co electrode with cobalt phosphate. Due to the unique properties of the cobalt phosphate, the constructed electrode exhibited favorable potentiometric responses for the determination of phosphate ion concentration. The sensing mechanism of this $H_2PO_4^-$-selective electrode was investigated in detail.

References

[1] F. Tafesse, M. Enemchukwu, Fabrication of new solid state phosphate selective electrodes for environmental monitoring, Talanta 83 (2011) 1491.

[2] R. De Marco, C. Phan, Determination of phosphate in hydroponic nutrient solutions using flow injection potentiometry and a cobalt-wire phosphate ion-selective electrode, Talanta 60 (2003) 1215.

[3] S. R. Crouch, H. Malmstadt, A Mechanistic investigation of molybdenum blue method for determination of phosphate, Anal. Chem. 39 (1967) 1084.

[4] K. Hayashi, T. Danzuka, K. Ueno, Spectrophotometric determination of phosphate using lanthanum chloranilate, Talanta 4 (1960) 244.

[5] B. Lopez-Ruiz, Advances in the determination of inorganic anions by ion chromatography, J. Chromatogr. A 881 (2000) 607.

[6] Z. Marczenko, Separation and spectrophotometric determination of elements, E. Horwood, 1986.

[7] D. Xiao, H.-Y. Yuan, J. Li, R.-Q. Yu, Surface-modified cobalt-based sensor as a phosphate-sensitive electrode, Anal. Chem. 67 (1995) 288.

[8] W.-H. Lee, Y. Seo, P. L. Bishop, Characteristics of a cobalt-based phosphate microelectrode for in situ monitoring of phosphate and its biological application, Sens. Actuators B 137 (2009) 121.

[9] Z. Chen, R. De Marco, P. W. Alexander, Floe-injection potentiometric detection of phosphates using a metallic cobalt wire ion-selective electrodes, Anal. Cmmun. 34 (1997) 93.

[10] L. Zhu, X. Zhou, H. Shi, a potentiometric cobalt-based phosphate sensor based on screen-printing technology, Front. Environ. Sci. Eng. 8 (2014) 945.

[11] R. De Marco, B. Pejcic, Z. Chen, Flow injection potentiometric determination of phosphate in wastes and fertilisers using a cobalt wire ion-selective electrode, Analyst 123 (1998) 1635.

[12] V. O. Ebuele, D. G. Congrave, C. D. Gwenin, V. Fitzsimmons-Thoss, Development of a cobalt electrode for the determination of phosphate in soil extracts and comparison with standard methods, Anal. Lett. 51 (2018) 834.

[13] P. Kumar, D. M. Kim, M.H. Hyun, Y.-B. Shim, An all-solid-state monohydrogen phosphate sensor based on a macrocyclic ionophore, Talanta 82 (2010) 1107.

[14] F. Tafesse, New solid state phosphate sensitive electrodes for routine environmental monitoring, J. Appl. Sci. 2 (2012) 128.

[15] M. R. Ganjali, P. Norouzi, M. Ghomi, M. Salavati-Niasari, Highly selective and sensitive monohydrogen phosphate membrane sensor based on molybdenum acetylacetonate, Anal. Chim. Acta 567 (2006) 196.

[16] A. K. Jain, V. Gupta, J. Raisoni, A newly synthesized macrocyclic dithioxamide receptor for phosphate sensing, Talanta 69 (2006) 1007.

[17] W. Liu, X. Li, M. Song, Y. Wu, A novel dibasic phosphate-selective electrode based on

Ferrocene-bearing macrocyclic amide compound, Sensors Actuators B: Chem. 126 (2007) 609.

[18] R. K. Meruva, M. E. Meyerhoff, Mixed potential response mechanism of cobalt electrodes toward inorganic phosphate, Anal. Chem. 68 (1996) 2022.

[19] W. H. Lee, Y. Seo, P. L. Bishop, Characteristics of a cobalt-based phosphate microelectrode for in situ monitoring of phosphate and its biological application, Sensors Actuators B: Chem. 137 (2009) 121.

[20] J. J. Wang, P. L. Bishop, Fabrication, calibration and evaluation of a phosphate ion-selective microelectrode, Environ. Pollut. 158 (2010) 3612.

[21] Y. Bai, J. H. Tong, C. Bian, S. H. Xia, Fabrication and characterization of cobalt nanostructure-based microelectrodes for phosphate detection, Key Engineering Materials, Trans Tech Publ. 483 (2011) 559.

[22] M. C. Sartori, T. R. Zezza, L. L. Paim, N. R. Stradiotto, Potentiometric determination of phosphorus in biodiesel using chemically modified electrode with cobalt film, Fuel 117 (2014) 564.

[23] [23] J. F. Ping, J. Wu, Y. B. Ying, Determination of Inorganic Phosphate in Environmental Water Using Cobalt Film Modified Ionic Liquid-Carbon Paste Electrode, Trans. ASABE 56 (2013) 779.

[24] D. Talarico, F. Arduini, A. Amine, D. Moscone, G. Palleschi, Screen-printed electrode modified with carbon black nanoparticles for phosphate detection by measuring the electroactive phosphomolybdate complex, Talanta 141 (2015) 267.

[25] Z. Chen, P. Grierson, M. A. Adams, Direct determination of phosphate in soil extracts by potentiometric flow injection using a cobalt wire electrode, Anal. Chim. Acta 363 (1998) 191.

[26] T. Kidosaki, S. Takase, Y. Shimizu, Electrodeposited Cobalt-Iron Alloy Thin-Film for Potentiometric Hydrogen Phosphate-Ion Sensor, J. Sensor Technol, 2 (2012) 95.

[27] R.C. Weast, Handbook of physics and chemistry, CRC Press, Boca Raton, 1983–1984, 1986.

[28] B. Boonchom, C. Danvirutai, Study of the dehydration of $Co(H_2PO_4)_2{\cdot}2H_2O$, J. Chem. Eng. Data 54 (2009) 1225.

[29] J. Chivot, L. Mendoza, C. Mansour, T. Pauporté, M. Cassir, New insight in the behaviour of Co–H 2 O system at 25–150 C, based on revised Pourbaix diagrams, Corros. Sci. 50 (2008) 62.

[30] J. Hanawalt, H. Rinn, L. Frevel, Chemical analysis by X-ray diffraction, Industrial & Engineering Chemistry Analytical Edition 10 (1938) 457.

Chapter2

Fabrication of a Phosphate Ion Selective Electrode Based on Modified Molybdenum Metal

A phosphate ion selective electrode using a molybdenum metal was constructed. The modified molybdenum electrode responded to HPO_4^{2-} in the presence of molybdenum dioxide and molybdophosphate ($PMo_{12}O_{40}^{3-}$) on the surface. The electrode exhibited a linear response to HPO_4^{2-} in the concentration range between 1.0×10^{-5} and 1.0×10^{-1} M (mol dm^{-3}) in the pH range from 8.0 to 9.5 with a detection limit of 1.0×10^{-6} M. The sensor showed a near Nernstian characteristics (–27.8±0.5 mV dec^{-1}) at pH 9.0. Since the responding potential was attributed to the activity of HPO_4^{2-}, the potential at a given concentration of phosphate depended on pH. The electrode indicated a good selectivity with respect to other common anions such as NO_3^-, SO_4^{2-}, Cl^-, HCO_3^- and CH_3COO^-. The modified molybdenum electrode can be continuously used over a 1 month with good reproducibility.

Introduction

Phosphate is considered as one of main components of ground and surface water, and it is also an essential nutrient for all plants [1-3]. In modern agriculture, phosphate is supplied to cultivate crops as an important fertilizer [4-6]. An excess release of phosphate derived from the fertilizer and a man-made waste to the natural environment however causes eutrophication [7-10]. The concentration control of phosphate based on the monitoring data is important in order to preserve the environment. On the other hand, it is important to evaluate the concentrations of phosphate in body fluids in clinical diagnosis of various disorders such as hyperparathyroidism, hypertension, deficiency of vitamin D, mineral and bone disorder and Franconia syndrome [11-14].

As for phosphate measurement, there are many analytical methods such as spectrophotometry, ion chromatography, flow injection analysis, and potentiometry [15-18]. Potentiometric evaluation of the concentration of phosphate using ion selective electrodes (ISEs) is one of prime candidates, since it is a fast, portable, simple, low cost and accurate analytical method [18-21]. Several phosphate ISEs constructed by metal|metal phosphate electrodes [22-27], surface modified electrodes [28] and liquid membrane electrodes [29] have been reported. It is well known that a cobalt electrode can respond to the concentration of dihydrogen phosphate [23-25]. However, the electrochemical properties of the ISE were unstable and the responding mechanism had not been clarified. Meruva and Meyerhoff suggested a mixed potential mechanism in the presence of oxide and dihydrogen phosphate [24]. The author's group successfully explained the responding mechanism based on the mixed potential of oxidation and phosphorylation of cobalt and proposed the best condition suitable for the measurement [25]. The

electrode showed a linear potential response in the concentration range from 1.0×10^{-1} to 1.0×10^{-6} mol dm^{-3} (M) in the pH range from 4.0 to 6.5. On the other hand, several research groups have reported that molybdenum electrodes can be used for the detection of monohydrogen phosphate (HPO_4^{2-}) around pH 8.0 [26,27]. Although the formation of molybdophosphate is involved in the potential response of the modified molybdenum electrode [27], the detailed mechanism remains to be clarified.

In the present study, the potential response of the modified molybdenum electrode to the concentration of HPO_4^{2-} and its pH dependence were examined. Based on the formation of molybdophosphate from molybdenum oxide and HPO_4^{2-}, the responding mechanism of the modified molybdenum electrode to the concentration of HPO_4^{2-} in the solution and optimum conditions for the detection of HPO_4^{2-} were investigated.

Experimental

Chemicals

Molybdenum wire (diameter: 2 mmϕ, length: 100 mm, 99.9%） was purchased from the Nilaco Co., Ltd. Molybdenum (IV) oxide, sodium dihydrogenphosphate (NaH_2PO_4), sodium hydrogenphosphate (Na_2HPO_4), sodium nitrate ($NaNO_3$), sodium chloride (NaCl), sodium sulfate (Na_2SO_4), sodium acetate (CH_3COONa), sodium hydrogencarbonate ($NaHCO_3$), and sodium hydroxide (NaOH) were purchased from Wako. Co. Ltd. Hydrochloric acid (HCl) was obtained from Kishida Co. Ltd. Phosphomolybdic acid hydrate ($H_3PMo_{12}O_{40}$•x-H_2O) was obtained from Tokyo Chemical Industry Co. Ltd. All chemical reagents were of analytical grade and were used without further purification.

Apparatus

Electrochemical measurements were conducted using an electrometer HE-106A (Hokuto Denko Co., Ltd.), a potentiostat/galvanostat HA1010mM1A (Hokuto Denko Co., Ltd.), a function generator HB305 (Hokuto Denko Co., Ltd.), and an A/D converter (GL900, Graphtec. Co., Ltd). The electrode surface before and after electrolysis treatment to modify the surface was observed by a field emission scanning electron microscope SU8000 (Hitachi High-Technologies Co.). By use of a pH meter PH-230SD (Lutron Co., Ltd. Taiwan), the pH of the solution was measured.

UV-Vis absorption spectra were observed using an UV-Vis spectrophotometer (UV-2550 (Shimadzu Co., Ltd). UV-Vis spectra of electrolyzed solutions were compared with those of a solution of phosphomolybdic acid hydrate ($H_3PMo_{12}O_{40}$•x-H_2O).

Preparation of Mo modified electrodes

In the potentiometric measurement of a modified molybdenum electrode as a phosphate-ion selective electrode, the surface of the molybdenum wire was polished by sandpapers of #80, #240, and

#1000, respectively. It was then washed within an ultrapure water for 30 min using an ultrasonic cleaner. The molybdenum wire was covered with a silicone tube except both ends of the electrode, and one end of the silicone tube was coated with epoxy resin to avoid the soakage of the solution into the gap. Thus, one end of the molybdenum wire was used as a working electrode. A platinum wire electrode was used as a courter electrode. The constant-potential electrodeposition was undertaken at +0.2 V vs. Ag|AgCl|sat. KCl in 0.1 M Na_2HPO_4 at pH 9 for about 2 h until the color of the electrode surface turned to black totally (coulomb cm^{-2}). After the electrolysis, the color of the electrolyzed solution changed yellow green. On the other hand, in the measurement of cyclic voltammograms, a molybdenum wire (outer diameter: 2 mmϕ) was inserted to a polytetrafluoroethylene (PTFE) material (inner diameter: 2 mmϕ), and the bare molybdenum electrode (surface area: 0.0314 cm^2) was used as a working electrode.

All potentiometric measurements were carried out in a two-electrode system using an Ag|AgCl|sat. KCl electrode and three phosphate-sensing electrodes (3 sets as parallel circuits). Cyclic voltammetry was carried out in a three-electrode system using the molybdenum electrode (a working electrode), an Ag|AgCl|sat. KCl electrode (a reference electrode) and a platinum wire electrode (a courter electrode).

Results and Discussion

Response characteristics of HPO_4^{2-}-ISE

Figure 1 illustrates the response characteristics of the modified molybdenum electrode to the total concentration of phosphate ion [Pi] at various pHs. In this case, the pH value of the phosphate solution was adjusted with NaOH and HCl solutions. The detection limit was 10^{-6} M in the pH region between 8.0 and 9.5. The modified molybdenum electrode showed a linear response with a slope of −27.8 ± 0.5 mV dec^{-1} to the concentration of monohydrogen phosphate ion ($[HPO_4^{2-}]$) in the range from 10^{-5} to 10^{-1} M at pH 9.0, where $[Pi] \approx [HPO_4^{2-}]$. The rest potential ($E_{ISE}$) of the modified molybdenum electrode used as an ion-selective electrode (ISE) at pH 9.0 was expressed by Eq. (2-1).

$$E_{ISE}\ (\text{pH } 9.0) = -(0.312 \pm 0.005)\ \text{V} - (0.0278 \pm 0.0005)\ \text{V} \times \log([\text{Pi}]/\text{M}) \qquad (2\text{-}1)$$

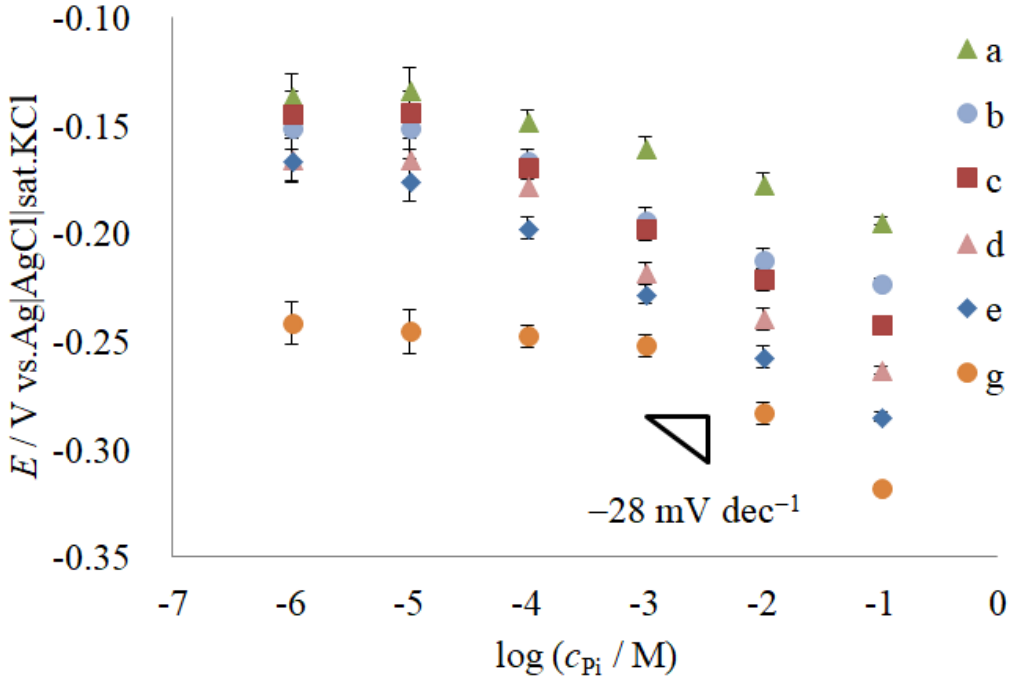

Fig. 1 Influence of pH on the potential response of the modified molybdenum electrode.
(a) pH 7.0, (b) pH 7.5, (c) pH 8.0, (d) pH 8.5, (e) pH 9.0 ,and (f) pH 9.5 and (g) pH 10.0.

Although the linear response was held in the region between pH 8.0 and pH 9.5, the rest potential at a given value of [Pi] decreased with an increase of pH. At pH 10.0, the detection limit increased around 10^{-3} M.

The pH dependence of the E_{ISE} value suggests that H^+ or OH^- is involved in the responding reaction to HPO_4^{2-}. Thus the E_{ISE} value depended on pH. The E_{ISE} value at $[HPO_4^{2-}] = 10^{-3}$ M was written by Eq. (2-2).

$$E_{ISE} = (0.0478 \pm 0.0005)\ \text{V} - (0.0308 \pm 0.0005)\ \text{V} \times \text{pH} \qquad (2\text{-}2)$$

The selectivity ($K_{B,A}^{pot}$) of the objective ion (B) to a coexisting ion (A) was evaluated at pH 9.0 by the mixed-solution method. The E_{ISE} value was represented by Eq. (2-3).

$$E_{ISE} = E' + \frac{RT}{n_B F} \ln\left(a_B + K_{B,A}^{pot}\, a_A^{\frac{n_B}{n_A}} \right) \qquad (2\text{-}3)$$

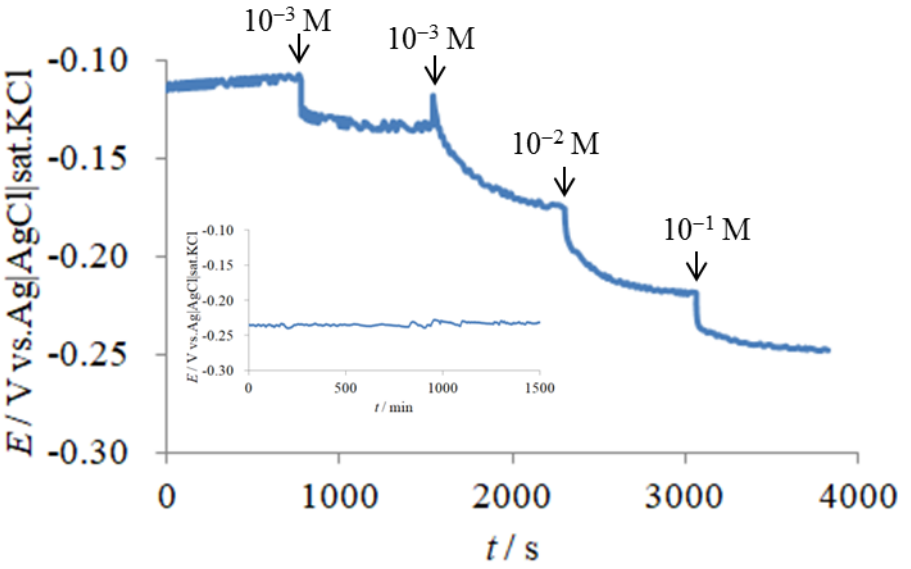

Fig. 2 Response time of the modified molybdenum electrode in Na_2HPO_4 solution at pH 9.0. Inset: Stability of the modified Mo electrode in 0.1 M NaH_2PO_4 solution at pH 9.0.

Here, E' is a constant value that depends on the identity of ionic species B (HPO_4^{2-}) and on the cell construction, n_A and n_B are the charge numbers of the ions A and B, F is the Faraday constant, a_A and a_B are the activities of ions A and B, R is the gas constant, and T is the temperature.

Table 1. Selective coefficients of the modified Mo electrode for other anions.

Anion	$\log K_{B,A}^{pot}$
NO_3^-	−3.5±0.2
Cl^-	−3.0±0.3
SO_4^{2-}	−2.0±0.3
HCO_3^-	−2.9±0.2
CH_3COO^-	−3.1±0.2

As shown in Table 1, all selectivity coefficients of common anions (NO_3^-, Cl^-, SO_4^{2-}, HCO_3^- and CH_3COO^-) were below –2; the modified molybdenum electrode showed a good performance on

selectivity. Figure 2 shows the dynamic response time of the modified molybdenum electrode. The response time was less than 5 min. As shown in the inset, the fluctuation of the potential was less than ± 5 mV within 24 h, and the properties remained unchanged one month after. When a bare molybdenum electrode was used as an ISE electrode, the responding potential was not constant in the begining and varied. But it gradually became to respond stably to [HPO_4^{2-}], as shown in Fig. 3(a). After the measurement (5 times observation), the color of the electrode surface was turned to dark brown. On the other hand, the responding characteristics of the modified electrode became stable, as shown in Fig. 3(b).

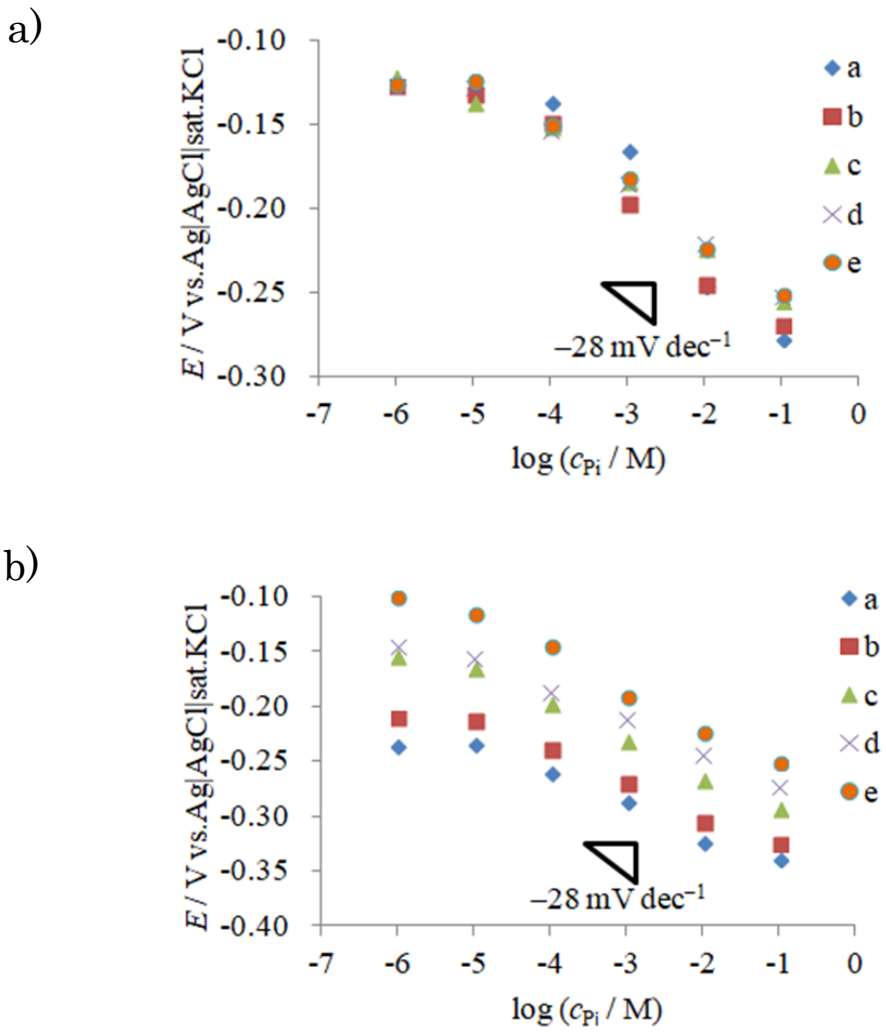

Fig. 3 Potential response characteristics in Na_2HPO_4 solution at pH 9.0 on (a) the Mo electrode and (b) the modified Mo electrode.

SEM images, XRD patterns of the deposit and UV-Vis absorption spectra

SEM images of the surface of both the bare and modified molybdenum electrodes were observed, as indicated in Fig. 4. The surface of the polished bare molybdenum electrode was smooth, while that of the modified molybdenum electrode was not smooth. Variously shaped crystals adhered to the surface of the electrode.

In order to construct a stable modified molybdenum electrode, the potential-controlled electrolysis was performed at 0.2 V vs. the Ag|AgCl|sat. KCl reference electrode for about 2 h. The color of the electrodeposit on the surface of the modified molybdenum electrode was dark brown and the electrodeposit was stripped off with a sand-paper. After the electrodeposit was dried, the XRD pattern of the electrodeposit was measured. As shown in Fig. 5, the main peaks of electrodeposit were identified to molybdenum and molybdenum dioxide (MoO_2).

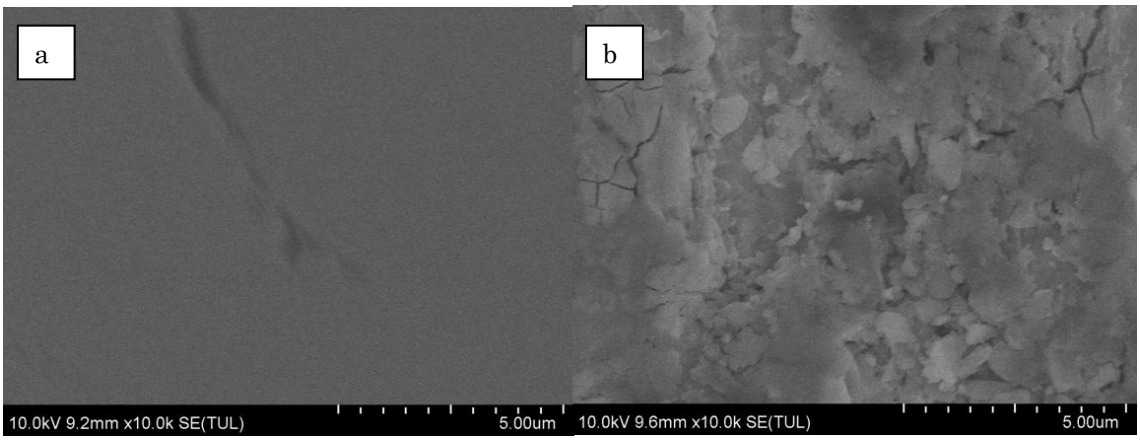

Fig. 4 SEM images of (a) the bare molybdenum electrode and (b) the modified electrode.

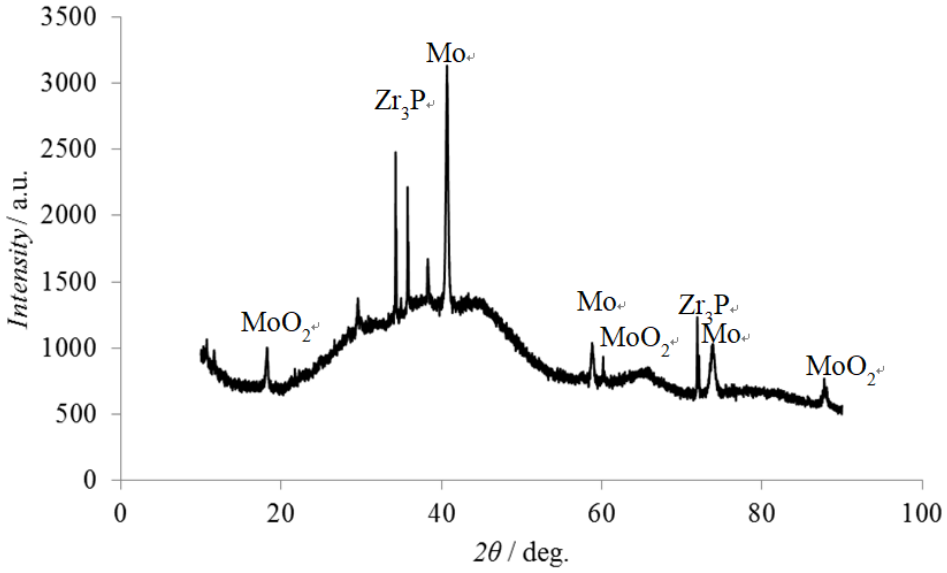

Fig. 5 XRD pattern of the electrodeposit on the surface of the modified Mo electrode.

When the molybdenum wire was electrolyzed at 0.2 V in 0.1 M Na_2HPO_4, the color of the electrolyzed solution was turned from colorless to yellow green. The solution was picked up and was diluted. The UV-Vis absorption spectrum of the diluted solution was observed as indicated by curve a in Fig. 6. Similarly, the UV-Vis absorption spectrum of 0.1 mM phosphomolybdic acid hydrate ($H_3PM_{12}O_{40}$•x H_2O) was measured (curve b). The spectra were overlapped with each other. The results clearly verify that $[PMo_{12}O_{40}]^{3-}$ was formed in the electrolyzed solution by the electrolysis.

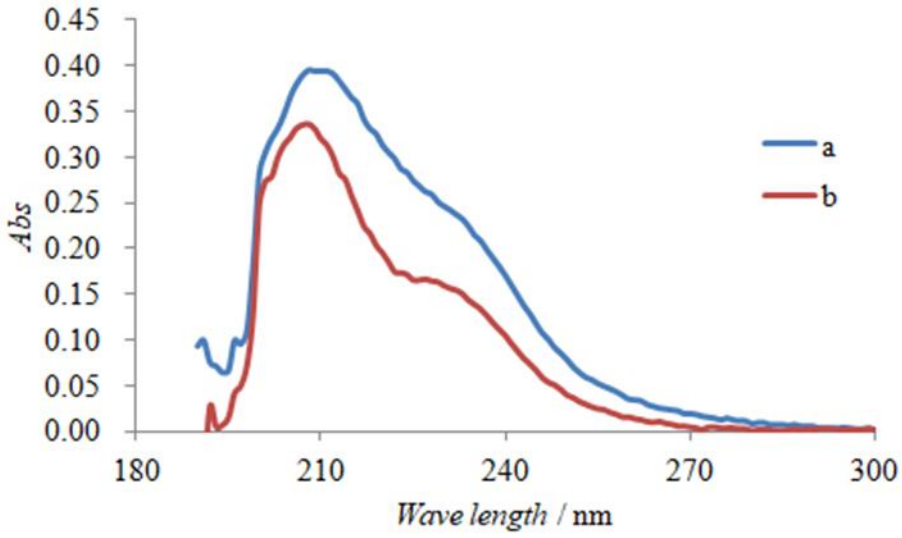

Fig. 6 UV-Vis absorption spectra of (a) the electrolyzed solution and (b) 0.01 mM phosphomolybdic acid hydrate.

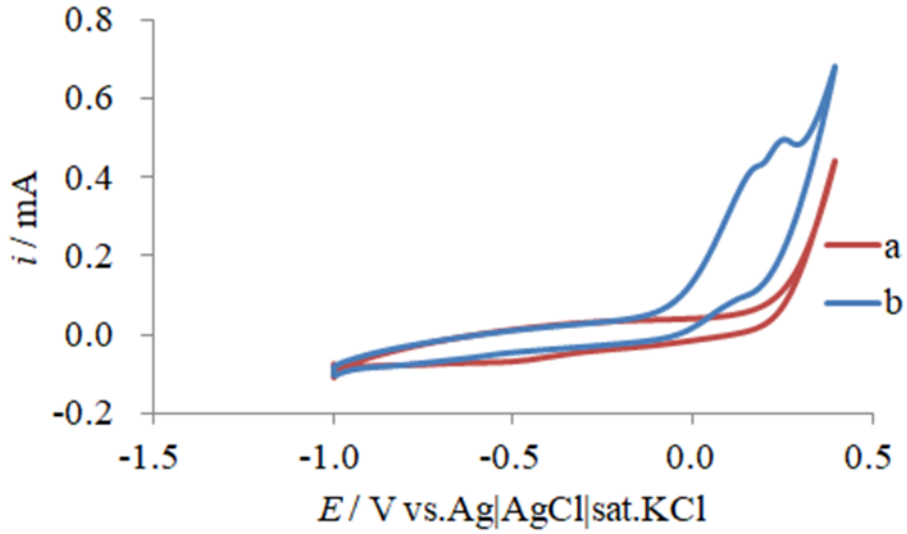

Fig. 7 Cyclic voltammagrams of a molybdenum metal electrode in 0.1 M NaCl (a) and 0.1 M NaH_2PO_4 (b) at pH 9.
Potential scanning rate: 50 mV s^{-1}. Electrode area: 0.0314 mm^2.

Electrochemical reaction on the surface of the molybdenum electrode

Fig. 7 shows cyclic voltammograms at a bare molybdenum electrode. Curves a and b were obtained in 0.1 M NaCl and 0.1 M Na_2HPO_4, respectively. The anodic current slightly flowed in the potential region more positive than –0.3 V. This would be caused by oxidation of molybdenum metal to MoO_2 based on the Pourbaix diagram, as shown in Fig. 8.[30] Above 0.25 V, the anodic current increased. The anodic waves might be attributed to the oxidation of MoO_2 to MoO_4^{2-}.[31,32] In addition, it has been reported that MoO_3 is formed by the reaction of MoO_2 with H_2O, as follows:

$$MoO_2 \rightarrow MoO_2^{+} + e^{-} \quad (2\text{-}4)$$

$$MoO_2^{+} \rightarrow MoO_2^{2+} + e^{-} \quad (2\text{-}5)$$

$$MoO_2^{2+} + H_2O \rightarrow MoO_3(s) + 2H^{+} \quad (2\text{-}6)$$

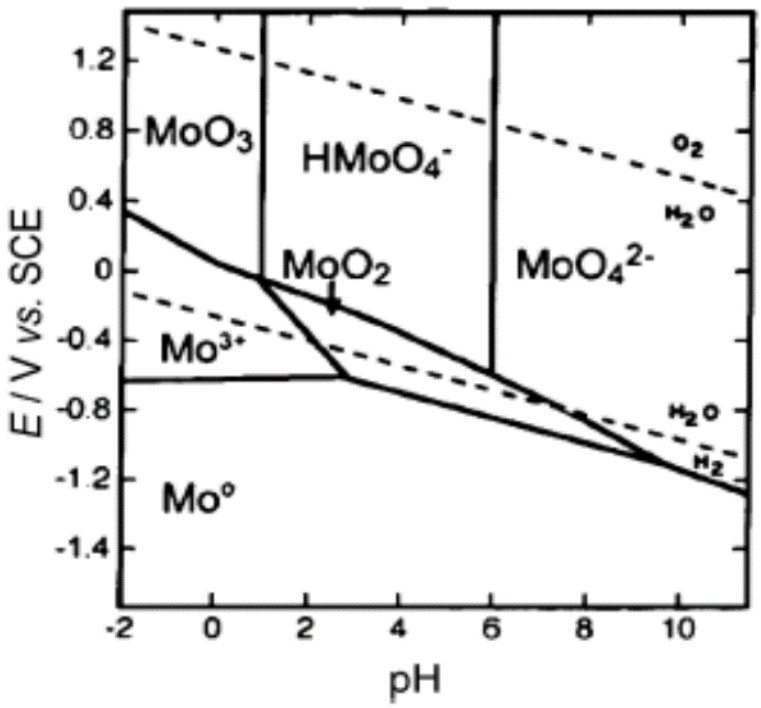

Fig. 8 Potential-pH diagram of a Mo-H_2O system *E* / V *vs.*NHE [30].

In the presence of HPO_4^{2-} in the aqueous phase, two anodic current peaks appeared around 0.15 V and 0.25 V, respectively. The anodic peaks seem to be caused by the reactions (4) and (5), respectively, facilitated by the reaction of MoO_3 and HPO_4^{2-}. In order to construct a stable modified-molybdenum electrode for the HPO_4^{2-}-ISE electrode, a bare molybdenum electrode was oxidized for about 2 h at 0.2 V. During the electrolysis, the color of the solution turned to yellow green. The wave form of the UV-Vis absorption spectrum (curve a in Fig. 6) of the electrolyzed solution obtained by the electrolysis was almost identical with that of the solution of phosphomolybdic acid ($12MoO_3 \cdot H_3PO_4$). This means that molybdophosphate ($PMo_{12}O_{40}^{3-}$) was formed by the electrolysis in the solution. Therefore, the reaction written below appear to occur on the electrode surface.

$$12MoO_3 + HPO_4^{2-} \rightarrow H^+ + PMo_{12}O_{40}^{3-} \qquad (2\text{-}7)$$

As shown in Fig. 5, a XRD pattern indicates the existence of MoO_2 alone on the surface of the modified molybdenum electrode. The broad peak around 25°-50° might be caused by other compounds such as MoO_3, $Mo(OH)_3$, and $Na_2HPMo_{12}O_{40}$. Since MoO_3 is not stable in the absence of H_2O, any clear peak to be assigned to MoO_3 was not observed.

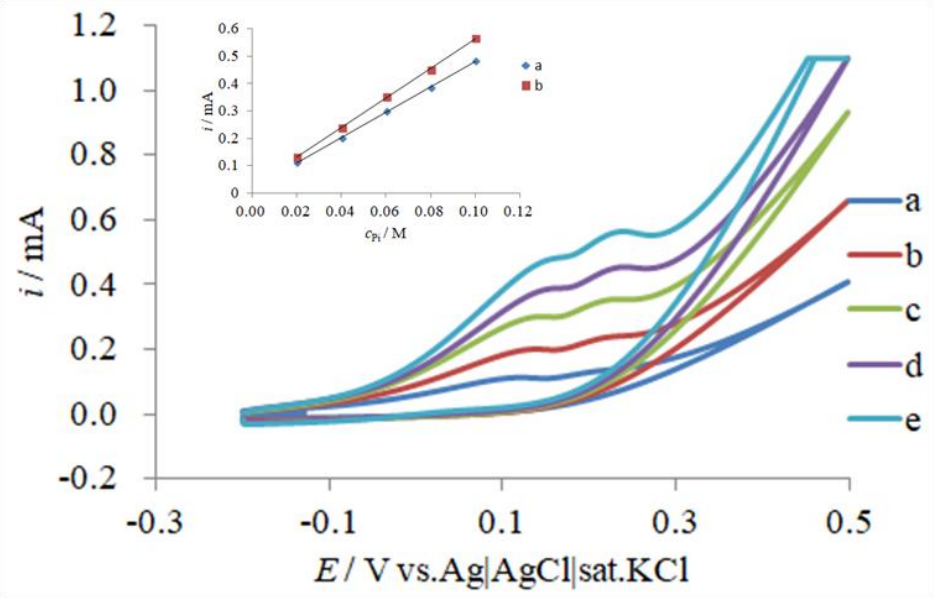

Fig. 9 Cyclic voltammograms of a molybdenum metal electrode in (a) 0.02 M, (b) 0.04 M, (c) 0.06 M, (d) 0.08 M, and (e) 0.10 M Na_2HPO_4 at pH 9.0.
Potential scanning rate: 50 mV s^{-1}. Electrode area: 0.0314 cm^2.
Inset: Concentration dependence of the cathodic peak current (I_p).

Fig. 9 indicates cyclic voltammograms of HPO_4^{2-} at the bare molybdenum electrode and its concentration dependence. The anodic peak currents (I_{pa} and I_{pb}) of peaks a (about 0.12 V) and b (about 0.23 V) were in proportion to [HPO_4^{2-}]. Thus, it is clear that the two anodic peaks are attributable to the reaction of molybdenum oxide and phosphate (probably HPO_4^{2-}). Although $PMo_{12}O_{40}^{3-}$ is soluble in aqueous phase, it is well known that $PMo_{12}O_{40}^{3-}$ adsorbs on the electrode surface [33, 34]. Since $PMo_{12}O_{40}^{3-}$ is adsorbed on the electrode surface in the present case, the rest potential seems to be stabilized. It is considered that the pH dependence of E_{ISE}, which is expressed by Eq. (2-2), is caused by the pH dependence of the oxidation of MoO_2 to MoO_3. The potential response became unstable below pH 7.5. This appeared to be ascribed to a decrease in the ratio of [HPO_4^{2-}]/ [$H_2PO_4^-$] based on the following relations [35];

$$H_2PO_4^- + H_2O \rightleftharpoons HPO_4^{2-} + H_3O^+, \quad (2\text{-}9)$$

$$K_{a2} = \frac{[HPO_4^{2-}][H_3O^+]}{[H_2PO_4^-]} = 6.23\times10^{-8} \ . \quad (2\text{-}10)$$

Figure 10 indicates cyclic voltammograms of HPO_4^{2-} at various pH values. Since [HPO_4^{2-}]/[Pi] at pH 7.0 and 7.5 are about 0.4 and 0.8, respectively, it is thought that the current heights at pH 7.0 and 7.5 were less than those at other pH values. Similarly, by considering the dissociation of HPO_4^{2-}

represented by Eqs. (2-11) and (2-12), it is predictable that the responding characteristics varies above pH 11.

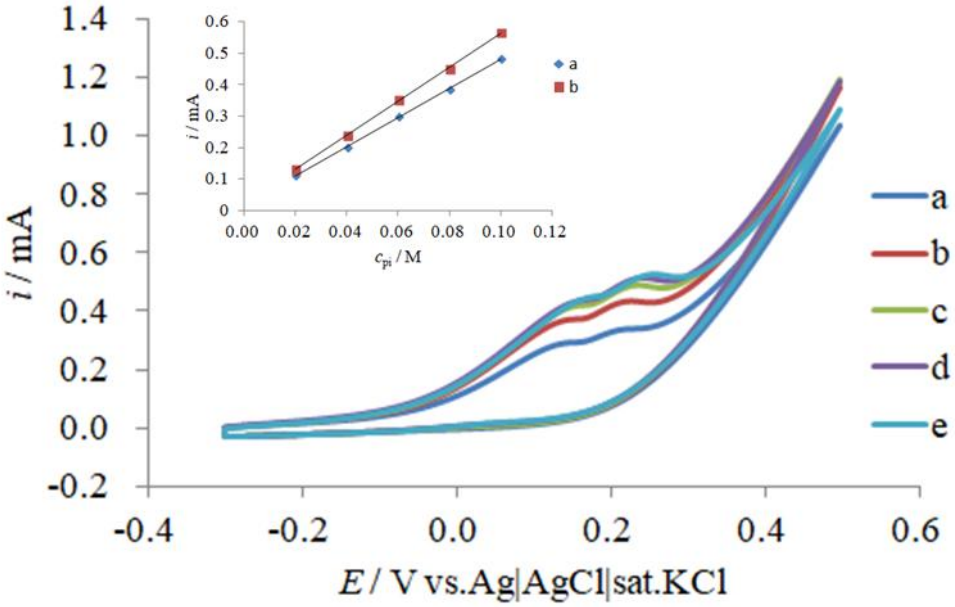

Fig. 10 Cyclic voltammograms of a molybdenum metal electrode in the presence of 0.1 M Na_2HPO_4 at various pH values: (a) pH 7.0, (b) pH 7.5, (c) pH 8.0, (d) pH 8.5, and (e) pH 9.0.
Potential scanning rate: 50 mV s^{-1}. Electrode area: 0.0314 cm^2.
Inset: HPO_4^{2-} concentration dependence of the cathodic peak current (I_p).

$$HPO_4^{2-} + H_2O \rightleftharpoons PO_4^{3-} + H_3O^+ \quad (2\text{-}11)$$

$$K_{a3} = \frac{[PO_4^{3-}][H_3O^+]}{[HPO_4^{2-}]} = 2.2\times10^{-13} \quad (2\text{-}12)$$

Considering the above relations, it is predicted that the modified molybdenum electrode can respond in the pH region between pH 8.0 and pH 11.0. Although the modified molybdenum electrode responded the concentration of HPO_4^{2-} at pH 10.0, the detection limit changed to 10^{-3} M. This might result from the change of the oxidation of MoO_2 judging from the Pourbaix diagram [30].

The cathodic peak-current in the cyclic voltammograms increased with an increase in pH of phosphate solutions. In the inset of Fig. 8, the horizontal ordinate shows the HPO_4^- concentration calculated on Eq. (2-11). There is a clear linear relationship between the HPO_4^{2-} concentration and the peak current.

Determination of phosphate concentration by the ISE method and comparison with the colorimetry method

Table 2 indicates phosphate concentrations in coca cola, nutrient solution, and waste water

determined by the present ISE method and the molybdenum blue colorimetric method.19 After the pH values of these samples were adjusted at 9.0, the phosphate concentrations were determined. The values determined by the present ISE method agreed with those by the molybdenum blue colorimetric method. On the other hand, the recovery measurement of phosphate in distilled water, tap water, and coca cola was performed. As shown in Table 3, it can be seen that the recovery was found to be 95 - 98 %, indicating that the present sensor was feasible to determine phosphate (HPO_4^{2-}) in real samples.

Table 2. Determination of phosphate in coca cola, nutrient solution and waste water

Sample	Mo-ISE（mM）	Colorimetry（mM）
Coca Cola	8.9 ± 0.2	9.1 ± 0.1
Nutrient solution	8.0 ± 0.2	8.3 ± 0.1
Waste water	1.0± 0.2	1.1 ± 0.2

Table 3. Recovery measurement of phosphate in distilled water, tap water, and coca cola.

Sample	Added （mM）	Found （mM）	Recovery rate（%）
Distilled water	10.0	9.8 ± 0.1	98
Tap water	10.0	9.8 ± 0.2	98
Coca Cola	10.0	9.5 ± 0.3	95

Conclusion

In this study, we designed stable modified-molybdenum electrode as a phosphate-ion selective electrode which can be used under mild-alkaline condition. The electrode showed a good performance responding to the logarithm of the relative concentration of phosphate ion ($HPO4^{2-}$) with a Nernstian slope. The electrode showed acceptable selectivity to common anions such as $SO4^{2-}$, $NO3^-$, Cl^- and so on. The responding mechanism can be explained by considering both the formation of molybdophosphate complexes including $PMo_{12}O40^{3-}$ from MoO3 and $HPO4^{2-}$ and the absorption of $PMo12O40^{3-}$ on the electrode surface. The feasibility of phosphate detection in real samples using the present electrode was proved.

References

[1] C.M. Mcgraw, S.E. Stitzel, J. Cleary, C. Slater, D. Diamond, Autonomous microfluidic system for phosphate detection, Talanta, 71(2007)1180-1185.

[2] C. Warwick, A. Guerreiro, A. Soares, Sensing and analysis of soluble phosphates in environmental samples: A review, Biosensors & Bioelectronics, 41(2013)1-11.

[3] P. Worsfold, I. McKelvie, P. Monbet, Determination of phosphorus in natural waters: A historical review, Analytica Chimica Acta, 918(2016)8-15.

[4] G. Nziguheba, E. Smolders, Inputs of trace elements in agricultural soils via phosphate fertilizers in European countries, 390(2008)53-57.

[5] K.G. Ragothama, Phosphate acquisition, Annu Rev Plant Physiol Plant Mol Biol, 97 (2005) 1087-1093.

[6] K.G. Raghothama, A.S. Karthikeyan, Phosphate Acquisition, Annual Review of Plant Physiology & Plant Molecular Biology, 274(2001)37-49.

[7] E.M. Bennett, S.R. Carpenter, N.F. Caraco, Human Impact on Erodable Phosphorus and Eutrophication: A Global Perspective, Bioscience, 51 (2009) 227-234.

[8] S.R. Carpenter, Eutrophication of Aquatic Ecosystems: Bistability and Soil Phosphorus, Proc Natl Acad Sci U S A, 102 (2005) 10002-10005.

[9] D. Conley, H.W. Paerl, R.W. Howarth, D.F. Boesch, S.P. Seitzinger, K.E. Havens, C. Lancelot, G.E. Likens, Eutrophication: Time to Adjust Expectations Response, 324 (2009) 723-725.

[10] J.R. Banu, S. Kaliappan, D. Beck, High rate anaerobic treatment of Sago wastewater using HUASB with PUF as carrier, International Journal of Environmental Science & Technology, 3(2006)77-87.

[11] P. Manghat, R. Sodi, R. Swaminathan, Phosphate homeostasis and disorders, Annals of Clinical Biochemistry An International Journal of Biochemistry & Laboratory Medicine, 51(2014)631-656.

[12] M. Copland, P. Komenda, E.D. Weinhandl, P.A. McCullough, J.A. Morfin, Intensive Hemodialysis, Mineral and Bone Disorder, and Phosphate Binder Use, American Journal of Kidney Diseases the Official Journal of the National Kidney Foundation, 68(2016)S24-S32.

[13] V.D. Lotte, W. Vincent, v.O.A. M., M.M.A. Q., P.R. C., Z.A. H., G. Henk, v.d.B. Cornelieke, M.K.A. C., K.W.K. H., Effect of a lifestyle intervention in obese infertile women on cardiometabolic health and quality of life: A randomized controlled trial, Plos One, 13 (2018)1-8

[14] G.W. Kim, J.E. Lin, A.E. Snook, A.S. Aing, D.J. Merlino, P. Li, S.A. Waldman, Calorie-induced ER stress suppresses uroguanylin satiety signaling in diet-induced obesity, Nutrition & Diabetes,9(2019)14-19

[15] G.F. Kirkbright, M. Marshall, Direct determination of phosphorus by atomic absorption flame spectrometry, Analytical Chemistry, 45(1973)1610-1613.

[16] P. Steinmann, W. Shotyk, Ion chromatography of organic-rich natural waters from peatlands III. Improvements for measuring anions and cations, Journal of Chromatography A, 706 (1995) 281-286.

[17] M. Ikejiri, T. Ohshima, A. Fukushima, K. Shimotohno, T. Maruyama, Synthesis and evaluation of 5′-modified 2′-deoxyadenosine analogues as anti-hepatitis C virus agents, 363(1998)191-199.

[18] A.T. Law al, S.B. Adeloju, Progress and recent advances in phosphate sensors: A review, Talanta, 114(2013)191-203.

[19] J.J. Wang, P.L. Bishop, Fabrication, calibration and evaluation of a phosphate ion-selective microelectrode, Environmental Pollution, 158(2010)3612-3617.

[20] S.O. Engblom, The phosphate sensor, Biosensors & Bioelectronics, 13(1998)981-994.

[21] S. Berchmans, T.B. Issa, P. Singh, Determination of inorganic phosphate by electroanalytical methods: A review, 7(2012)729.

[22] F. Tafesse, M. Enemchukwu, Fabrication of new solid state phosphate selective lectrodes for environmental monitoring, 83(2011)1491-1495.

[23] D. Xiao, H.-Y. Yuan, J. Li, R.-Q. Yu, Surface-Modified Cobalt-Based Sensor as a Phosphate-Sensitive Electrode, Analytical Chemistry, 67(1995)288-291.

[24] R.K. Meruva, M.E. Meyerhoff, Mixed potential response mechanism of cobalt electrodes toward inorganic phosphate, Analytical Chemistry, 68 (1996) 2022-2026.

[25] K. Xu, K. Yuki, K. Kenji, S. Osamu, Phosphate ion sensor using a cobalt phosphate coated cobalt electrode, Electrochimica Acta, 282(2018)242-246.

[26] H.X. Li, R.X. Wang, X.R. Li, G. Tao, W. Ying, S.X. Guo, L.P. Sun, Z.Y. Yang, X.J. Yang, W.P. Jiang, Increasing DHA and EPA Concentrations Prolong Action Potential Durations and Reduce Transient Outward Potassium Currents in Rat Ventricular Myocytes, 46 (2010) 163-169.

[27] D. Talarico, F. Arduini, S. Cinti, A. Amine, G. Palleschi, Screen-printed electrode modified with the carbon black nanoparticles as a cost-effective and sensitive sensor for phosphate detection, Proceedings of the 2015 18th AISEM Annual Conference, AISEM 2015, 2015.

[28] P.R. Moses, R.M. Harnden, J.Q. Chambers, Electrochemical oxidation of multisulfur heterocycles reactions of dithiane cations in acetonitrile, Chemischer Informationsdienst, 84 (1977) 187-194.

[29] F. Kivlehan, W.J. Mace, H.A. Moynihan, D.W.M. Arrigan, Study of electrochemical phosphate sensing systems: Spectrometric, potentiometric and voltammetric evaluation, Electrochimica Acta, 54(2009)1919-1924.

[30] V.S. Saji, P.C.-W. Lee, Molybdenum, Molybdenum Oxides, and their Electrochemistry, 5(2012)1146-1152.

[31] P. Wang, L.L. Wilson, D.J. Wesolowski, J.r. Rosenqvist, A. Anderko, Solution chemistry of Mo(III) and Mo(IV): Thermodynamic foundation for modeling localized corrosion, Corrosion

Science, 52(2010) 1625-1634.

[32] M.N. Hull, On the anodic dissolution of molybdenum in acidic and alkaline electrolytes, Journal of Electroanalytical Chemistry, 38 (1972) 143-157.

[33] H.K. Nejad, F. Najafi, A. Soleimani-Gorgani, Encapsulation of flexible organic light emitting diodes by UV-cure epoxy siloxane, Journal of Applied Polymer Science, 136 (2019)427-437

[34] A.G. Fogg, N.K. Bsebsu, Differential-pulse voltammetric determination of phosphate as molybdovanadophosphate at a glassy carbon electrode and assessment of eluents for the flow injection voltammetric determination of phosphate, silicate, arsenate and germanate, 106 (1981) 1288-1295.

[35] T. Tanaka, M. Miura, T. Ishiyama, ADSORPTIVE VOLTAMMETRIC DETERMINATION OF ORTHOPHOSPHATE AT A GLASSY CARBON ELECTRODE, Journal of Trace & Microprobe Techniques, 19(2001)591-599.

Chapter3

Electrochemical pH Sensor Based on a Hydrogen-storage Palladium Electrode with Teflon Covering to Increase Stability

A pH responsive electrode was fabricated using hydrogen (H_2) storing palladium (Pd). The Pd electrode stores H_2 generated electrochemically at suitable potentials. Although the Pd electrode is usually unstable due to the release of H_2, the stability dramatically increased by coating the Pd electrode with a Teflon tube. After the Pd electrode was coated with palladium hydride (PdH_x) on its surface, the resting potential of the modified Pd electrode responded to changes in the pH with a near Nernstian response of -56.2 ± 0.2 mV pH^{-1} in the range from pH 1 to pH 13. It was stabilized by covering with a Teflon tube and reused by the electrolysis. As H_2 gas is spontaneously released from the modified Pd electrode, the partial pressure of H_2 gas on the surface of the Pd electrode is almost constant (H_2 gas is almost saturated in the vicinity of the electrode). Accordingly, the potential is assumed to be determined by the pH value of the aqueous solution based on the redox potential of the $H_2|H^+$ couple. When the pH value of the objective solution is almost constant, the modified Pd electrode can serve as a reference electrode without leakage of the inner electrolyte as in the Ag|AgCl|sat. KCl electrodes.

Introduction

In various aqueous solutions, the pH is represented as a negative common logarithm depicting the activity of protons in aqueous solution. The pH value is one of the most important indicators of the chemical forms of the solute and the chemical and/or biochemical reactions occurring in this environment. The pH measurement is required for determination of chemical characteristics, and several measuring methods such as color change indicators [1], potentiometry (quinhydrone electrodes [2], glass electrodes [3], hydrogen (H_2-)generating electrodes [4], metal oxide electrodes [5], liquid-membrane type or film-type proton (H^+)-selective electrodes [6], etc.), and amperometry [7] have been previously reported.

Although the pH measurement using acid/base indicators is simple, easy and inexpensive, monitoring is not suitable because it requires the periodic sampling or checking by pH-indicator dyes. Additionally, the quinhydrone electrode is not ideal for monitoring method because it requires the addition of a reagent to the cell system [2]. H_2-generating electrodes using elements such as platinum and palladium (Pd) have often been used as reference or pH-sensing electrodes [8]. However, their application has been very uncommon because of its difficulty in safety treatment of H_2 gas. Several solid electrodes such as metal oxides and metal hydrides have been also previously reported as pH sensors [9-12]. Metal hydrides such as palladium hydride (PdH_x) are particularly attractive because the electrode potentials are determined by the spontaneous release of H_2 gas from the hydrides. However, they are not widespread

because of their instability. As for metal oxides, the potential is unstable because the electrode reaction is caused by multiple reactions. Conversely, the glass electrode is the most popular pH-sensing system because of its simplicity, ease of use, and stability [2]. However, it is fragile and difficult for miniaturization. The alkaline error also influences the pH detection to some extent. In case of a proton-selective electrode, the detection range is much smaller than that of other methods (H_2-generating electrodes, metal oxide electrodes and the glass electrode) [13].

In the present study, a pH responsive electrode with hydrogen-storing palladium was improved and the mechanism of the pH response of the Pd electrode were investigated in detail. Properties such as the response, selectivity, stability and acid/alkaline error of the Pd electrode were described to evaluate the properties of the Pd electrode as a pH sensor that is tough and easy to miniaturize. As the Pd electrode does not release harmful substances and is also renewable by electrolysis to generate H_2 gas, it can be applied as an alternative device for on-site monitoring in medical, agriculture, food, and engineering fields. Furthermore, the Pd electrode can be used as a reference electrode, if pH of the objective solution is almost constant.

Experimental

Reagents

All solutions were prepared using UL-PURE water (Komatsu Electronics. Co., Ltd., Japan) with a resistivity of 18.2 MΩ cm at 25 ˚C. HCl, KCl, NaCl, LiCl, potassium hydrogen phthalate (KHP), di-sodium hydrogen phosphate, sodium bicarbonate and sodium hydroxide were purchased from Wako. Co., Ltd. (Japan). A Pd rod (outer diameter: 2 mm, length: 100 mm, 99.9%) was obtained from Nilako Co., Ltd. (Japan). All the chemicals were reagent grade and were used without further purification.

Instruments and Fabrication

Potentiometric measurements were conducted using an electrometer HE-106A (Hokuto Denko Co., Ltd., Japan). Cyclic voltammograms were measured by use of a potentiostat/galvanostat HA1010mM1A (Hokuto Denko Co., Ltd., Japan), a function generator HB305 (Hokuto Denko Co., Ltd., Japan), and an A/D converter GL900, (Graphtec Co., Ltd., Japan).

Electrolysis was carried out using a potentiostat/galvanostat HA1010mM1A (Hokuto Denko Co., Ltd., Japan). One end of the Pd metal rod was sealed by a Teflon tubular rod (outer diameter: 10 mm, inner diameter: 2 mm, and length: 20 mm, SANPLATEC Co., Ltd., Japan), and was consecutively polished with sandpapers of #80, #240, and #1000 grit, and with alumina abrasive filaments (1 μm in diameter). Furthermore, the rod was washed for 30 min in an ultrasonic cleaner. The modified Pd electrode was prepared by the potential controlled electrolysis at −0.9 V in a 0.1 M HCl solution. H_2 gas was generated on the surface of the Pd electrode, as shown in Fig. 1. Because the H_2 bubbles were

covered with the surface of the Pd electrode, the current decreased, as indicated in Fig. 2 and finally became 0 A. This operation was repeated several times until the electrolysis coulomb number reached to 2.5 C.

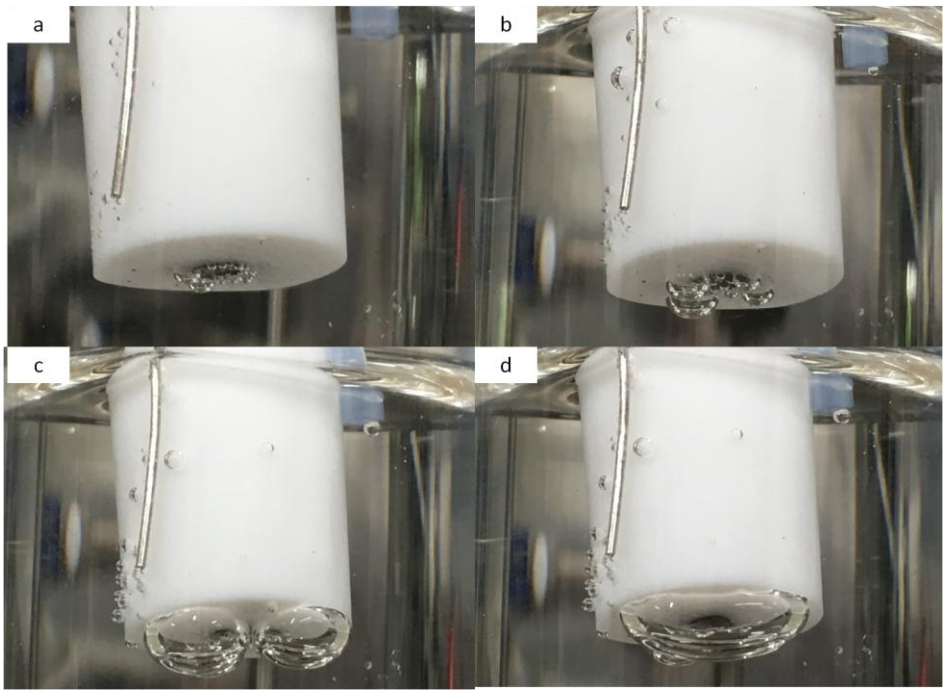

Fig. 1 Photographs of the palladium electrode taken during the electrolysis (−0.9 V). Photographs (a), (b), (c), and (d) correspond to the arrowed conditions in Figure S2.

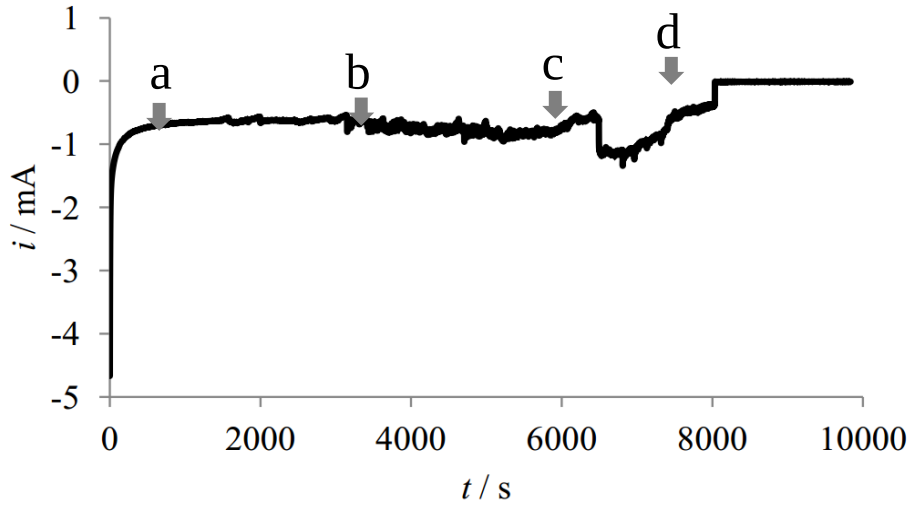

Fig. 2 Current fluctuation during electrolysis at −0.9 V. The photographs in Fig. S1 were taken at points a–d.

Potassium tetraphenylborate (KTPhB) was synthesized by the following steps: First, 10 mL of 0.1 M NaTPhB was mixed with an aqueous solution containing excess KCl, and the mixture was stirred for 2 h. The precipitated KTPhB was isolated by filtration and washed with distilled water. The precipitate was dried at 50 °C under vacuum. A liquid-membrane type K^+-ISE was prepared as follows. A responsive membrane was prepared by drying a THF solution (1.5 mL) containing 0.04 g of valinomycin, 0.4 g of KTPhB, 0.152 g of PVC, and 0.304 g of o-NPOE. The end of a pipette tip (1 mL) was cut and the membrane was attached at the cross-section of the pipette tip. Then, 1.5 mL of 0.1 M KCl was placed in the pipette tip and an Ag|AgCl electrode was inserted. The structure and appearance of the K^+-ISE are shown in a previous work [1]. Electrometrical measurements were carried out with a two-electrode system using two reference electrodes (Ag|AgCl|sat. KCl and the modified Pd electrodes) and the K^+-ISE.

Electrochemical Measurements.

Cyclic voltammograms were obtained using a three-electrode cell system. A Pd electrode, a platinum wire, and an Ag|AgCl|sat. KCl electrode were used as the working, counter and reference electrodes, respectively. Potentiometric measurements for pH-sensing were conducted by a two-electrode cell system. The modified Pd electrode and the Ag|AgCl|sat. KCl electrode were utilized as the pH-sensing and reference electrodes, respectively. Potentiometric measurements of K^+ concentration by use of a K^+ ion-selective electrode (K^+-ISE) were also carried using the modified Pd and Ag|AgCl|sat. KCl electrodes as reference electrodes.

Microscopy

Microscopic images were obtained using a field emission scanning electron microscope (FE-SEM, SU8000, Hitachi High-Technologies, Japan). The accelerating voltage was 1 kV.

Results and Discussion

pH Detection

The resting potential of the unmodified Pd electrode was not affected by the pH, and had a value of about +0.1 V. After the storage of H_2 by the electrolysis, the Pd electrode responded to the pH value of the test solution. Fig. 3 illustrates the dynamic response characteristics of the unmodified and the modified Pd electrodes in the pH range from 1 to 13. Here, the buffer reagents used are specified in Table 1.

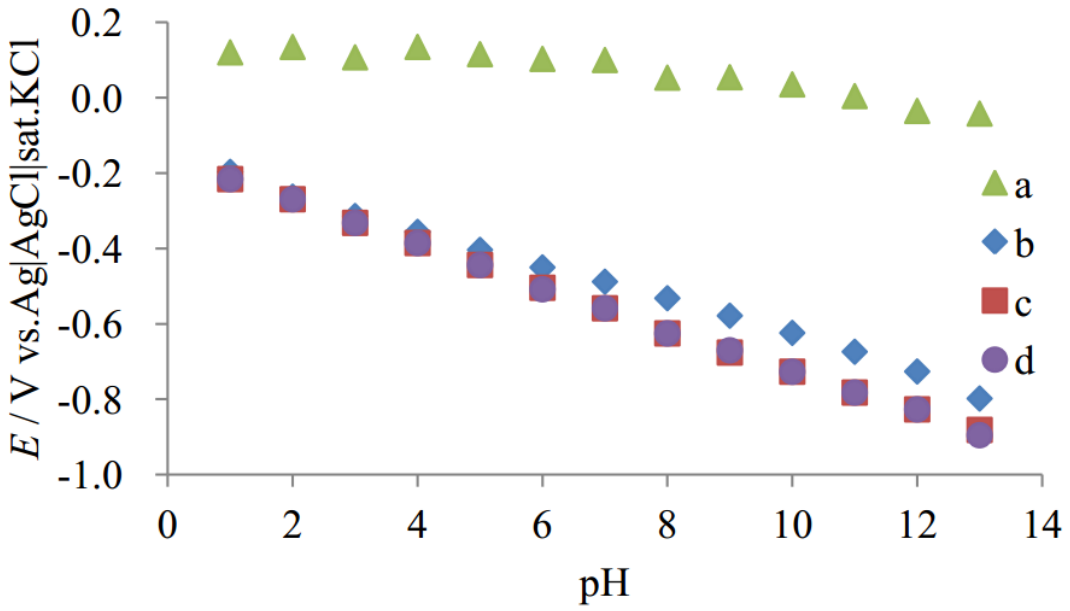

Fig. 3 The relation between the resting potential of the modified palladium electrode and pH. Coulomb number by the electrolysis: (a) 0C, (b) 0.5 C, (c) 2.5 C, and (d) 5.0 C.

Table 1. Test buffer solution at various pH

pH	Buffer solution
1–2	HCl
3–6	KHP
7–8	PBS
9–11	$NaHCO_3$
12–13	NaOH

To store H_2 gas into the Pd electrode, a potential of –0.9 V was applied to the Pd electrode. The Pd electrode whose coulomb number was 0.5 C (◆) exhibited a response to the concentration of protons with a slope of –47.0 ± 0.2 mV pH^{-1}. When the electric charge increased to 2.5 C (■), the slope increased to –56.2 ± 0.2 mV pH^{-1} mV pH^{-1}. When the coulomb number became 5 C (●), the slope was approximately maintained at the same value. Thereafter, the constant potential electrolysis was conducted by applying 0.5 V to remove H_2 from the Pd electrode. After the decomposition of PdH_x, the Pd electrode lost the response properties to the protons in the test solution (▲). Thus, the existence of

PdH_x was essential for the response mechanisms of protons. The Pd electrode that was electrolyzed to 5 C is hereafter referred to as the modified Pd electrode. The ideal resting potential of the H_2-generating electrode ($\Delta\phi$ (H)) is expressed by

$$\begin{aligned}\Delta\phi_e(\mathrm{H}) &= \Delta\phi_e^{\circ} - \frac{RT}{2F}\ln\frac{P(\mathrm{H_2})/P^{\circ}}{a_{\mathrm{H^+}}{}^2} \\ &= \Delta\phi_e^{\circ} - \frac{RT}{2F}\ln\frac{P(\mathrm{H_2})}{P^{\theta}} + \frac{RT}{F}\ln a_{\mathrm{H^+}} \\ &= \Delta\phi' - 0.0591\mathrm{pH}\end{aligned} \tag{3-1}$$

Here, $\Delta\phi$ (H) is the standard potential of the redox reaction of the $H_2|H^+$ couple, R is the gas constant, T is the temperature, $P(H_2)$ is the partial pressure of H_2 in the aqueous solution, P^{θ} is the standard pressure, a_{H^+} is the activity of proton in the aqueous solution, and $\Delta\phi'$ is a constant value. The modified Pd electrode responded to the pH value from 1 to 13 with a slope of about −56.2 ± 0.2 mV pH^{-1}. In particularly, the slope was -58.1 ± 0.2 mV pH^{-1} in the pH region from 1 to 9. Considering the activity of H^+ based on the Debye-Hückel limiting law, the slope in the pH region from 1 to 13 was −57.2 ± 0.2 mV pH^{-1}. Then, the slope in the pH region from 1 to 9 was −60.0 ± 0.2 mV pH^{-1}. The slope was an almost Nernstian response. The practical response experiment was conducted from pH 13 to pH 1.

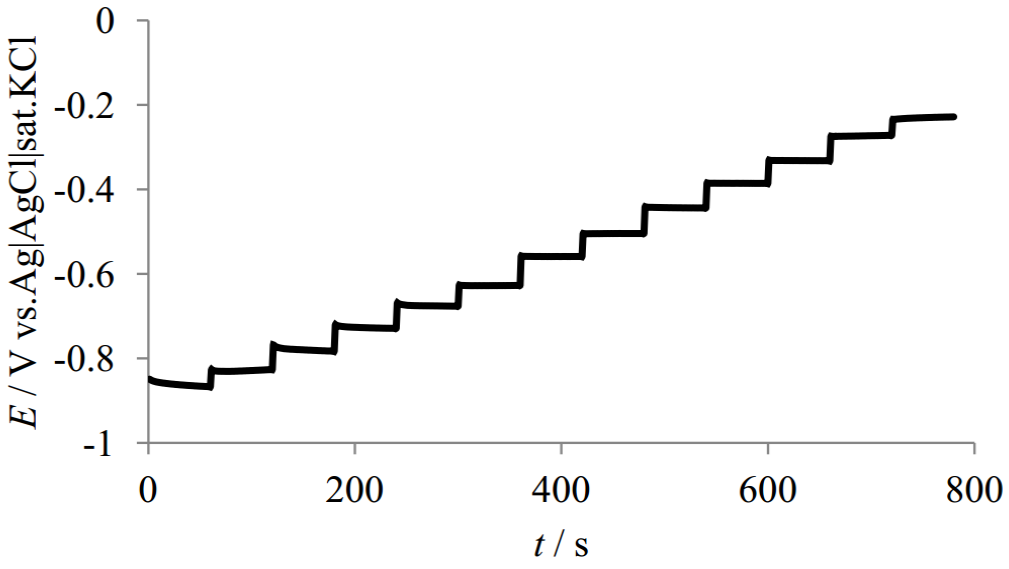

Fig. 4 Response time of the modified palladium electrode on increasing the pH from 1 to 13.

As shown in Fig. 4, the response time was less than 5 s. The potential fluctuations at pH 1, 7, and 13 at 25 ˚C were contained within ±2 mV during 24 hours, as shown in Fig. 5. When the modified Pd electrode was used in phosphate buffer solution (pH 7) for three weeks, the potential changed by less than 5 mV. In this case, the Teflon tube covered with the modified Pd electrode was prevented the release of hydrogen from the modified Pd electrode, as shown in Fig. 6. Although the potential of the modified Pd electrode covered with the Teflon tube was almost constant, that in the absence of the Teflon tube varied in no time.

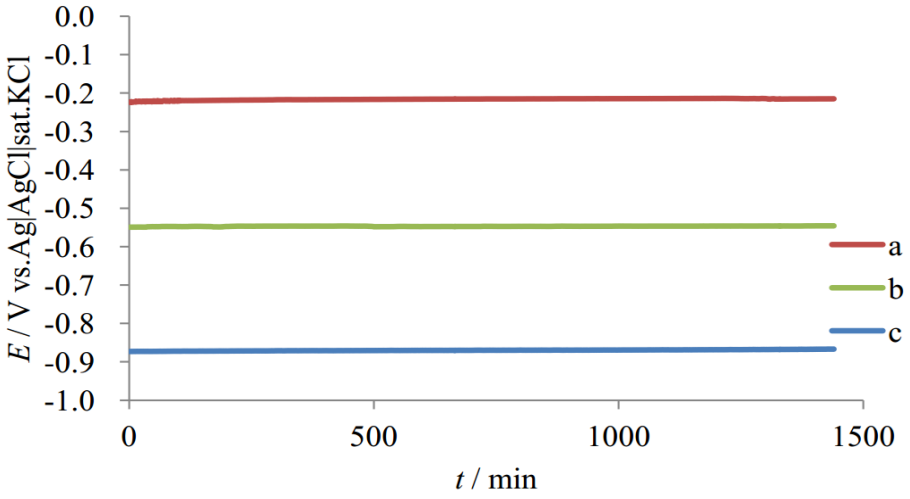

Fig. 5 Stability of the modified palladium electrode for 24 hours: (a) pH 1, (b) pH 7, (c) pH 13.

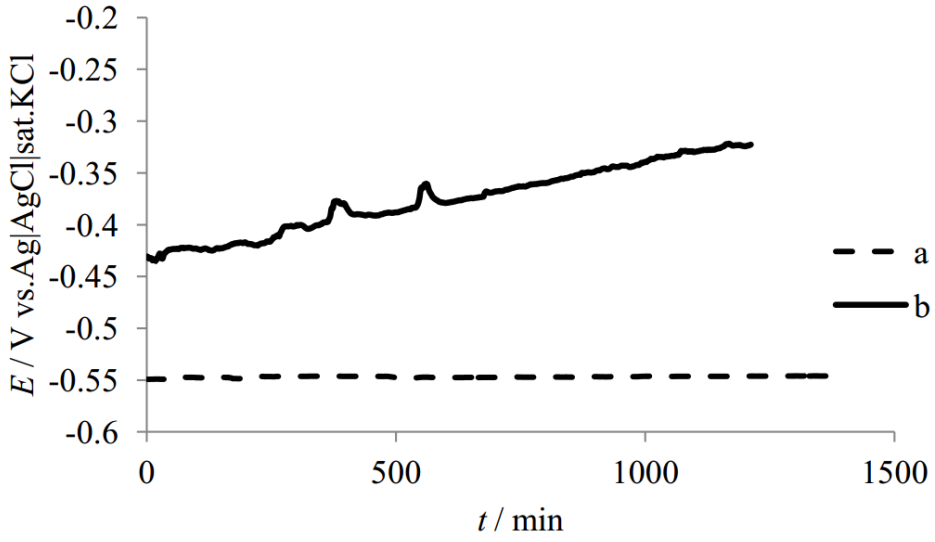

Fig. 6 Time-courses of the resting potentials of the palladium hydrogen storage electrode covered with the Teflon tube (a) that without the Teflon tube (b) at pH 7.

a)

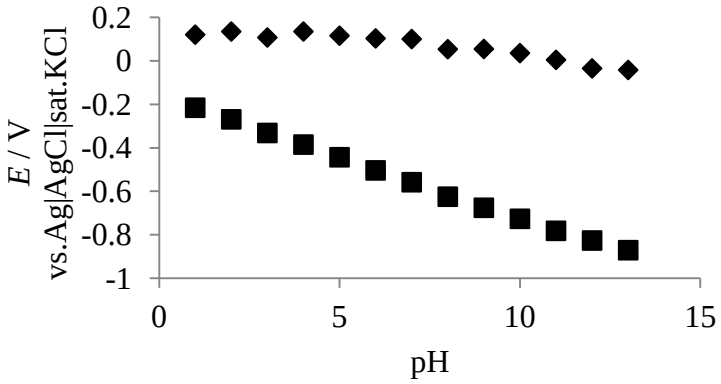

b)

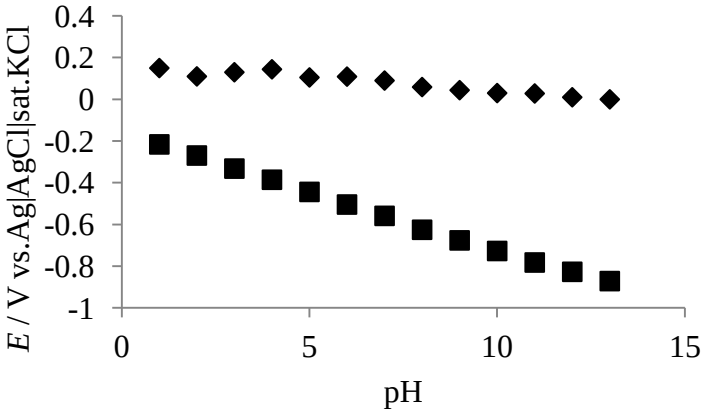

c)

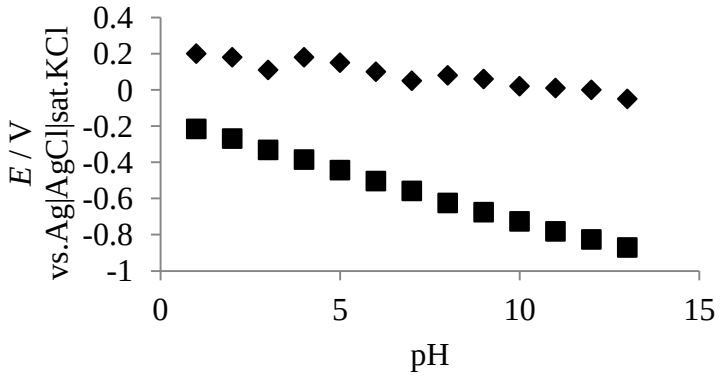

Fig. 7. Potential responses of the modified and unmodified palladium electrode to pH (■: the hydrogen storage electrode, ◆: the metal electrode without hydrogen) in the case of (a) first cycle, (b) second cycle, and (c) third cycle of the repetition of the electrolysis. The hydrogen storage electrode was prepared by the electrolysis at –0.9 V to be 2.5 C. The metal electrode without hydrogen was made by the electrolysis at 0.5 V to release hydrogen gas.

Fig. 7 exhibits the potential responses when the modified Pd electrode was repeatedly prepared. The potential responses of the first prepared modified Pd electrode and the Pd metal electrode after H_2 was removed is shown in Fig. 7a as a first cycle. Similarly, the potential responses of second and third cycles are indicated in Figs. 7b and 7c. Because the modified Pd electrode can resurge by the electrolysis, it is very useful as a pH electrode or a reference electrode.

Scanning Electron Microscopy (SEM) images

Fig. 8 shows the SEM images at the surface of the bare Pd electrode before and after the electrolysis. The surface of the Pd electrode had smooth and homogenous exterior before the electrolysis. After the electrolysis with a coulomb number of 2.5 C, the SEM image shows the electrode surface coated with crystals with a diameter of about 1 μm. The electrodeposits would be assigned to PdH_x.

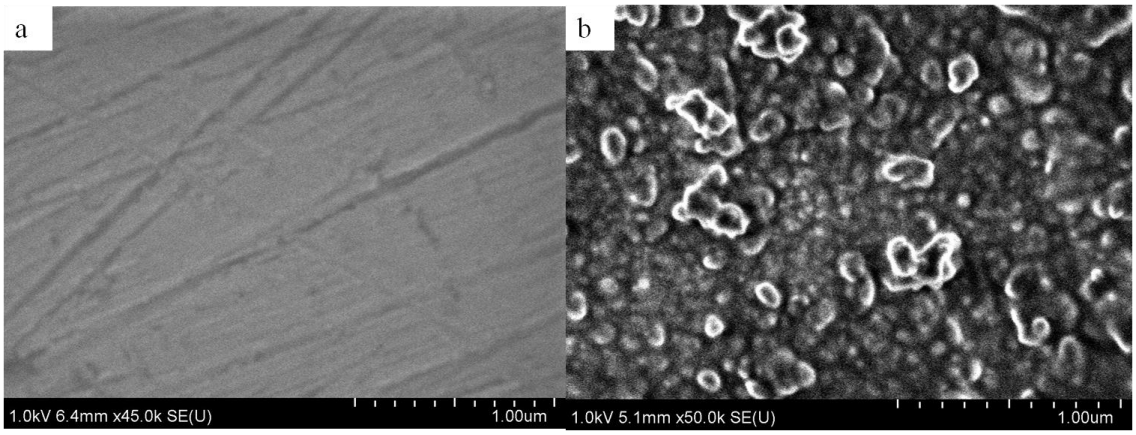

Fig. 8. SEM images of the palladium electrode before (a) and after (b) electrolysis.

A)

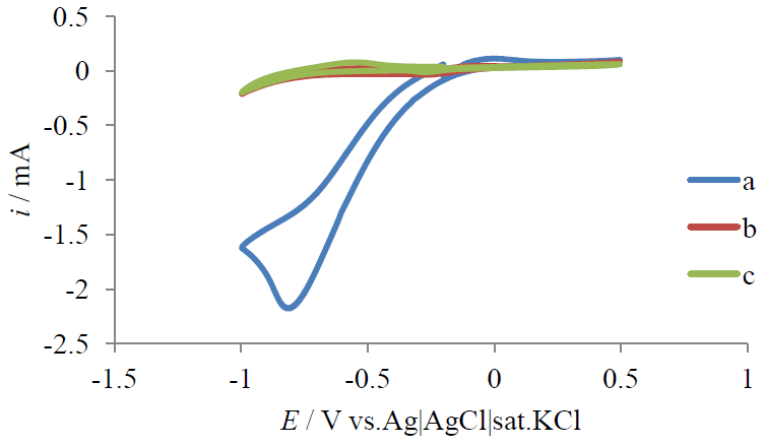

B)

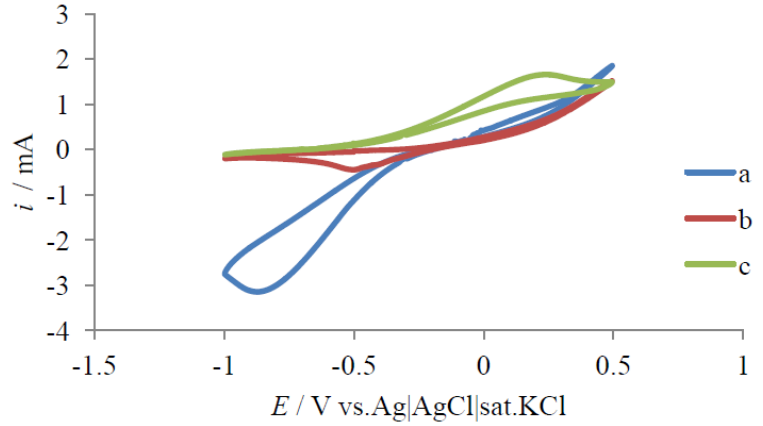

Fig. 9 Cyclic voltammograms of the palladium electrode in solutions of various pH values (A) before and (B) after the electrolysis. Electrolyte solution: (a) 0.1 M HCl (pH 1); (b) 0.1 M NaCl (pH 7); (c) 0.1 M NaOH (pH 13).

Electrochemical Reaction

Fig. 9 indicates the cyclic voltammograms obtained at pH 1, 7, and 13. A large cathodic peak was observed at about –0.8 V in 0.1 M HCl (pH 1). This cathodic peak was caused by the reduction of H^+ to H_2 [14]. In this case, a part of the H_2 gas generated by the reduction of H^+ was stored into the Pd electrode and PdH_x seemed to be formed (Eq 2).

$$Pd + x/2\ H_2 = PdH_x \qquad (3\text{-}2)$$

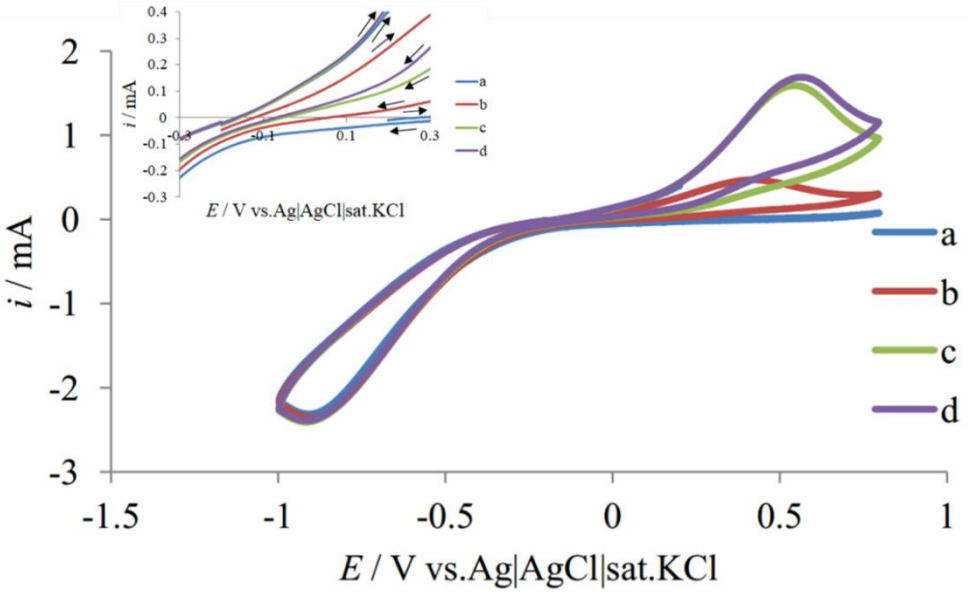

Fig. 10 Cyclic voltammograms of the palladium electrode in 0.1 M HCl at the potential scanning rate of 0.05 V s^{-1}. (a) First cycle; (b) second cycle; (c) third cycle; and (d) fourth cycle. Inset: enlarged graph of the potential region between –0.3 and 0.1 V. (a) First cycle; (b) second cycle; (c) third cycle; and (d) fourth cycle.

At pH 7 and 13, the cathodic peak currents decreased with a decrease in the concentration of H^+ in the aqueous solution. Since the cathodic peak height was proportional to the concentration of HCl, as shown in Fig. 9, it is evident that the cathodic wave at –0.8 V was caused by the reduction of H^+ to H_2

Fig. 10 shows 4 cycles of cyclic voltammograms observed in 0.1 M HCl using the unmodified Pd electrode. The initial potential was –0.2 V, and the potential was scanned between 0.8 V and –1.5 V at a scan rate of 0.05 V s^{-1}. An anodic current wave was not observed in the first cycle. However, an anodic peak appeared at 0.5 V after the second cycle. As the redox potential of the $H_2|H^+$ couple in 1 M HCl (pH 0) was –0.2222 V, it seems that the cathodic peak was caused by both the release of H_2 gas from the modified Pd electrode and the oxidation of H_2 to H^+ [14]. Therefore, the anodic wave was not observed at the first cycle, and was observed due to the formation of PdH_x layers after the second cycle. The zero-current potential shifted about 0.1 V in the negative direction, as indicated by the inset of Fig. 10. After the electrolysis to store H_2 gas in the Pd electrode, the modified Pd electrode was washed and dried. Then, the Pd electrode expanded out of the Teflon insulant. When H_2 gas was released from the modified Pd electrode, the constant-potential electrolysis at 0.5 V was conducted. During the electrolysis, numerous bubbles of H_2 gas were observed (Fig. 11) and the expanded part of the modified Pd electrode returned to its original state.

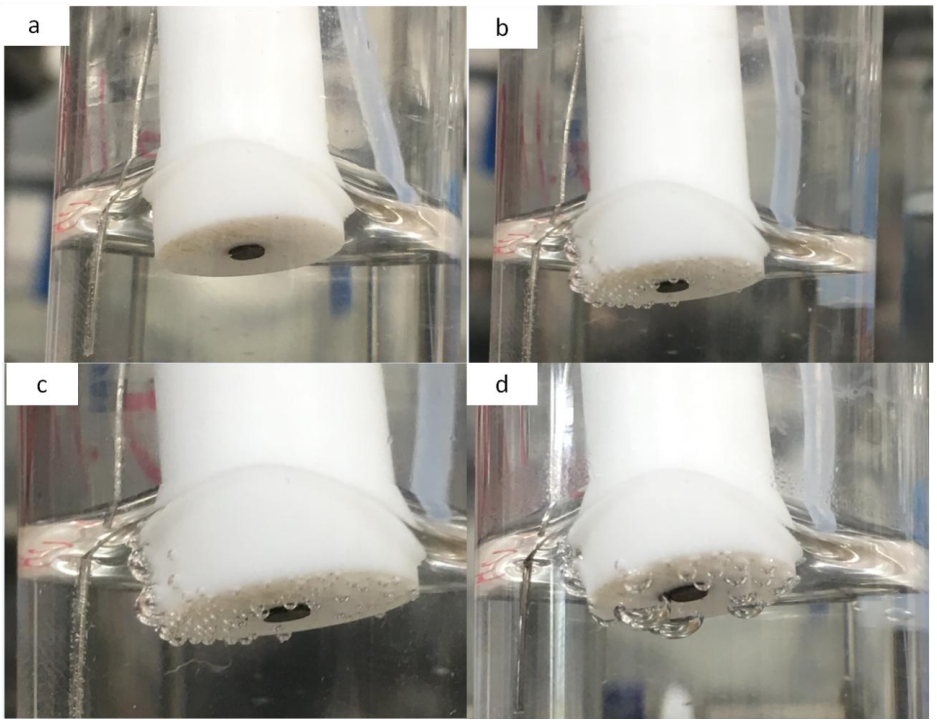

Fig. 11 Photographs of the modified palladium electrode during the electrolysis at 0.5 V. Length of the electrolysis: (a) 0 min; (b) 5 min; (c) 20 min; (d) 60 min.

The cathodic peak around 0.5 V is believed to be caused by the release of H_2 gas from the modified Pd electrode and the oxidation of H_2 to H^+. In addition, the height of the cathodic peak decreased after the third cycle. Thus, the redox potential of the $H_2|H^+$ couple was determined at about −0.2 V at pH 1. The height of the cathodic peak observed around −0.9 V was proportional to the square root of the potential scanning rate and to the concentration of H^+, as shown in Figs. S7 and S8, which implied that the reaction was controlled by the diffusion of H^+.

Electrolysis was carried out applying −0.9 V in a 0.1 M HCl solution. H_2 gas was generated on the surface of the palladium electrode, as shown in Fig. 1. Because the H_2 bubbles were covering the surface of the palladium electrode, the current decreased, as shown in Fig. 2. The current finally fell to 0 A (indicated by arrow d) due to full coverage. This operation was repeated several times until the electrolysis coulomb number reached 2.5 C. The potential response was observed from pH 13 to pH 1, as shown in Fig. 4. Fig. 5 shows the potential fluctuations at pH 1, 7, and 13 at 25 °C.

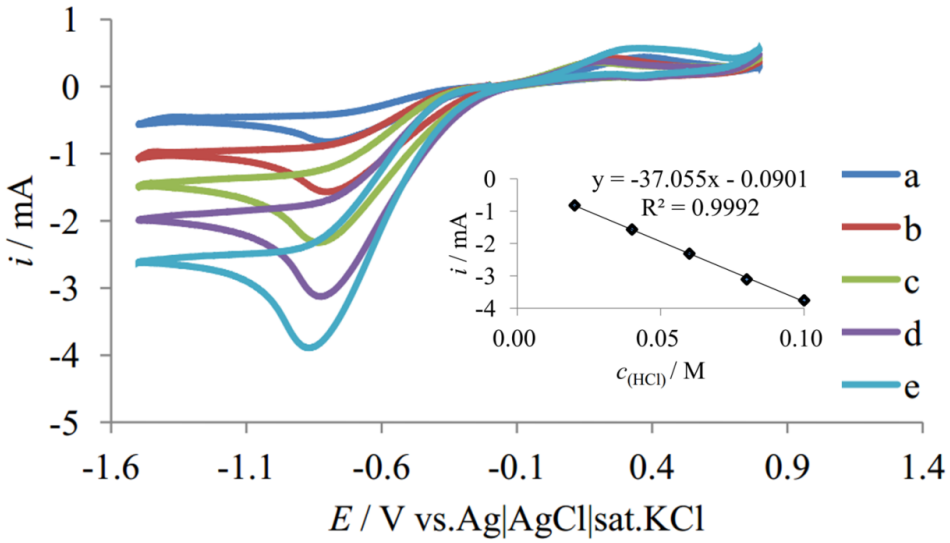

Fig. 12 Cyclic voltammograms of the modified palladium electrode in solutions containing various concentrations of HCl at a potential scan rate of 0.05 V s−1. HCl concentration: (a) 0.02 M; (b) 0.04 M; (c) 0.06 M; (d) 0.08 M; (e) 0.10 M. Inset: peak heights of the cyclic voltammograms.

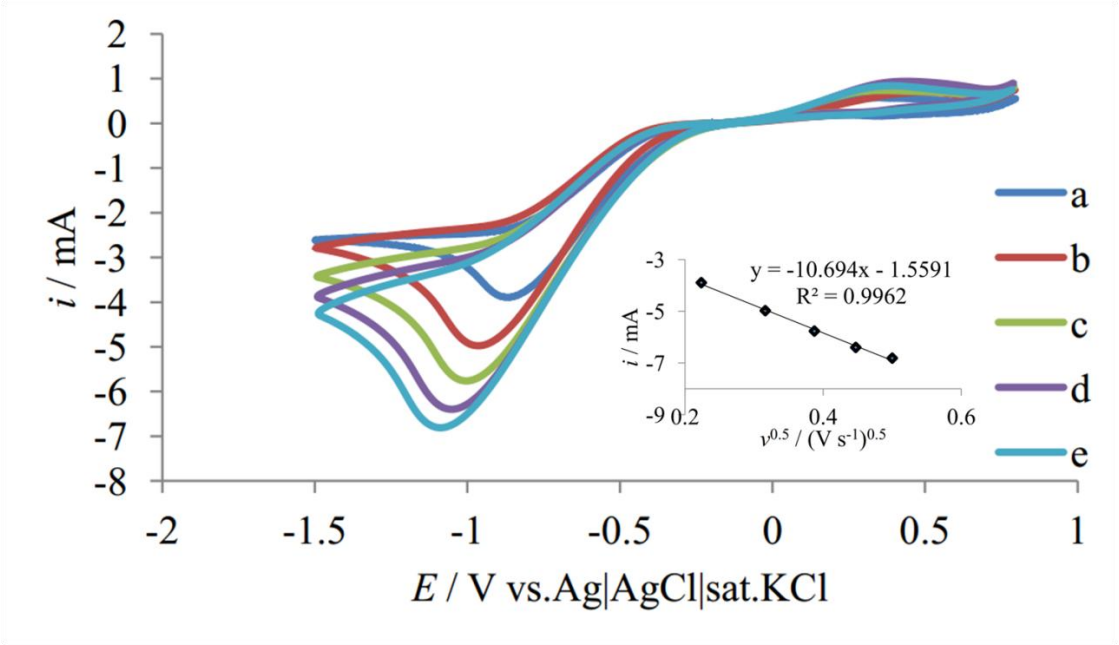

Fig. 13 Cyclic voltammograms of the modified palladium electrode in 0.1 M HCl solution at various potential scan rates: (a) 0.05 V s^{-1}; (b) 0.10 V s^{-1}; (c) 0.15 V s^{-1}; (d) 0.20 V s^{-1}; (e) 0.25 V s^{-1}. Inset: peak current of cyclic voltammograms of a bare palladium electrode at various potential scan rates in 0.1 M HCl.

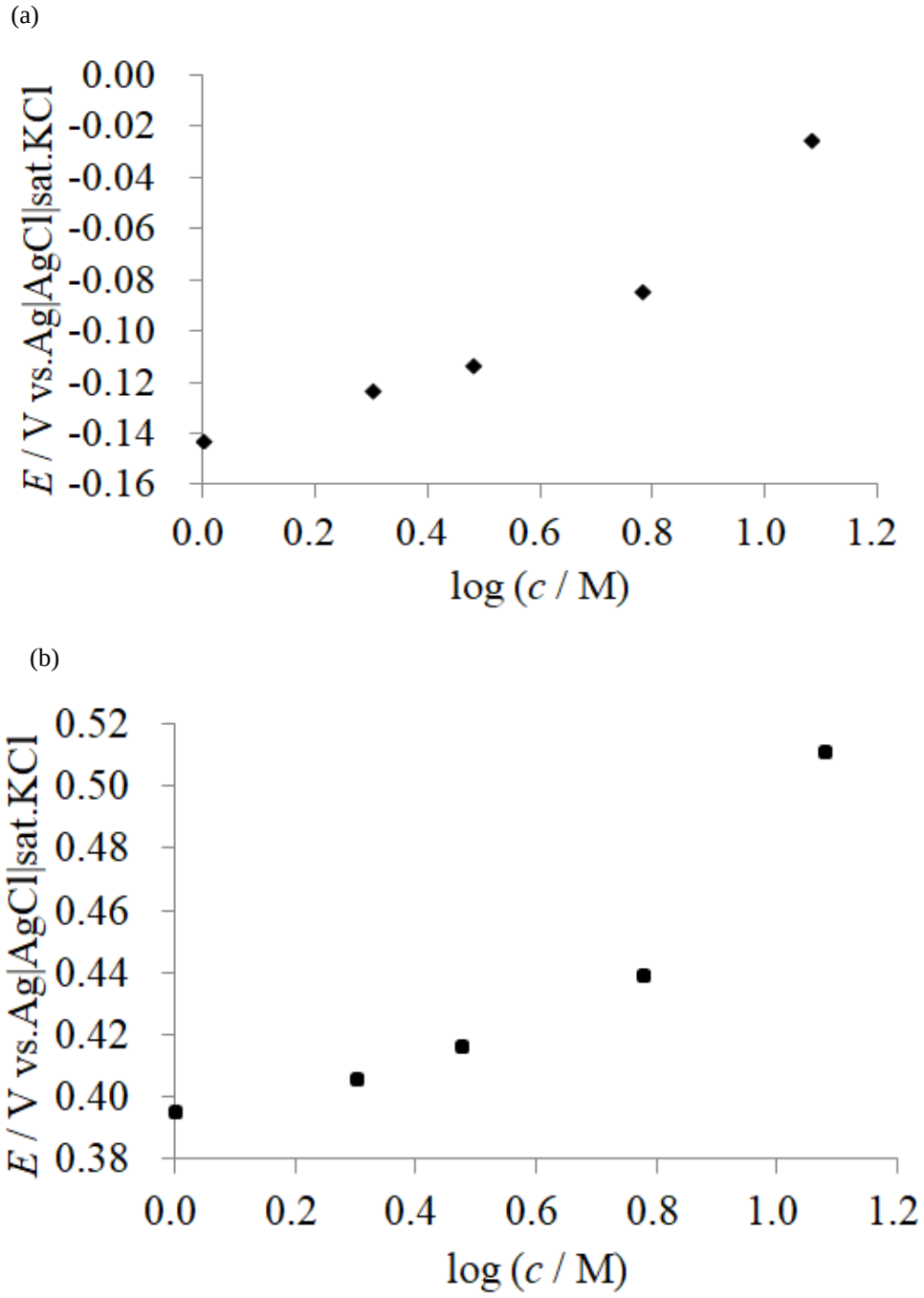

Fig. 14 Acid error in the case of the modified palladium electrode in the HCl solution(a); cid error in the case of the glass electrode(b).

Fig. 9A shows the cyclic voltammograms obtained at pH 1, 7, and 13 before the electrolysis. A large cathodic peak was observed at about −0.8 V in the case of pH 1 (0.1 M HCl). The peak height of the cathodic peak caused by the reduction of H^+ to H_2 depended on the pH. Since the cathodic peak height was proportional to the concentration of HCl, as shown in Fig. 12, it is clear that the cathodic peak

observed around –0.8 V was caused by the reduction of H^+ to H_2. On the other hand, a couple of anodic and cathodic peaks appeared around –0.3 V in all cases using the modified Pd electrode, as shown in Fig. 9B. These anodic reactions were caused by both the release of H_2 gas from the modified palladium electrode and the oxidation of H_2 to H^+ on the palladium electrode. Fig. 11 shows photographs taken during the electrolysis. As the electrolysis progressed, several bubbles of hydrogen gas were observed. The height of the cathodic peak observed around –0.9 V was proportional to the square root of the potential scanning rate, as shown in Fig. 13, indicating that the reaction was controlled by the diffusion of H^+.

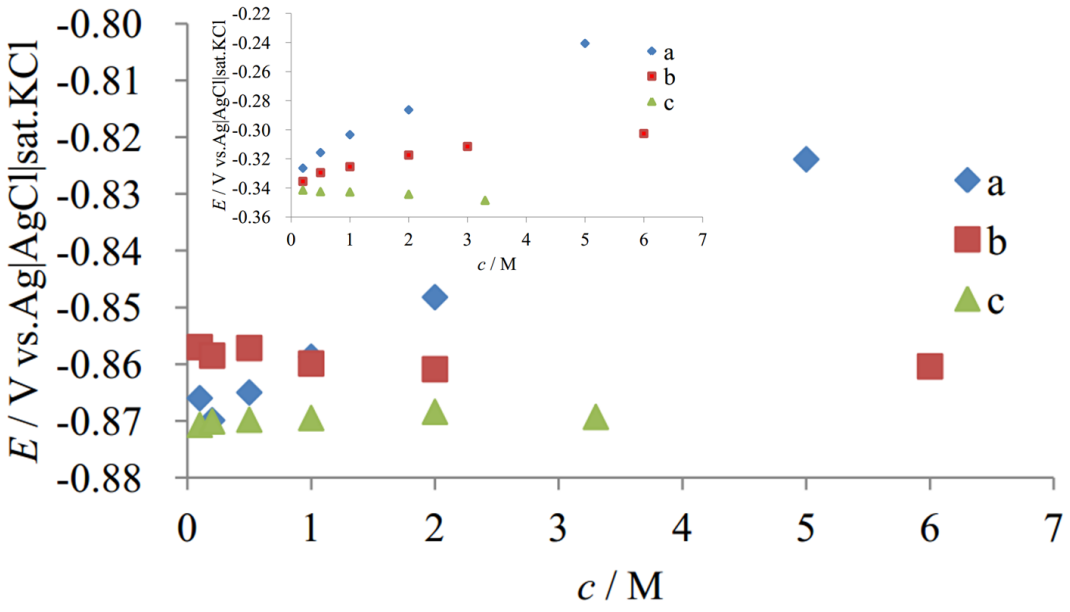

Fig. 15 Alkaline error in the case of the modified palladium electrode in various chloride solutions containing (a) Li^+, (b) Na^+, and (c) K^+. Inset: Alkaline error in the case of the glass electrode. (a) Li^+; (b) Na^+; and (c) K^+.

Acidic and Alkaline Errors

Acidic and alkaline errors of the modified Pd electrode were investigated. In the concentration of HCl ranging from 1 M to 12 M, the resting potential shifted in the positive direction in comparison with the calculated values, as illustrated in Fig. 6. Darrell et al. reported that the potential change in the case of the glass electrode as a pH meter increased with a decrease in the pH value bellow pH 0 [15]. The modified Pd electrode implied the same trend as the glass electrode, as shown by the inset of Fig. 6.

Regarding the alkaline error, the influence on the pH value was observed in the presence of Li^+ when the concentration of Li^+ was higher than 1 M, as illustrated in Fig. 15. This can be attributed to the formation of the Li–Pd alloy ($PdLi_7$) [16]. The displacement in the case of the modified Pd electrode was

less than the half of that in the case of the glass electrode. In contrast, the effect of the pH value was not observed in the presence of K^+ and Na^+. In the case of glass electrode, the alkaline error appeared in the presence of any alkaline metal ions at concentrations higher than 0.1 M. When the concentration of Na^+ or K^+ is higher than 0.1 M in all systems, the modified Pd electrode was superior to the glass electrode as the pH-sensing electrode. That is to say, we can measure the pH value by use of the modified Pd electrode more accurate than by use of the glass electrode.

Real sample monitoring

Table 2 indicates pH values of various fluids evaluated by use of the glass and the modified Pd electrodes. These are in good agreement with each other and almost compatible with reported values [17-23]. In addition, calibration curves of the K^+-ISE were obtained by use of the modified Pd and Ag|AgCl|sat. KCl electrodes as the reference electrodes. When the modified Pd electrode was used as a reference electrode, it is proved that the modified Pd electrode can be practically used, as shown in Fig. 16.

Table 2. pH values of various fluids [17-23]

Solution	Glass electrode	Pd modified electrode	Reported value
Calpis	3.63±0.05	3.96±0.06	3.3 [17]
Milk	6.67±0.03	6.08±0.08	6.4 [18], 7.0 [19]
Vinegar	2.85±0.05	2.49±0.07	2.9 [19]
Soy sauce	3.48±0.04	3.46±0.08	4.8 [20]
Nutrient solution	6.91±0.05	6.65±0.05	6.2 [21]
Coca-Cola	2.79±0.03	2.86±0.03	2.37±0.03 [22], 2.74±0.01 [23]
Coca-Cola Zero	2.86±0.03	2.77±0.06	2.96±0.03 [23]
Drinking yogurt	3.90±0.03	3.34±0.03	4.6 [19], 3.83±0.03 [23]

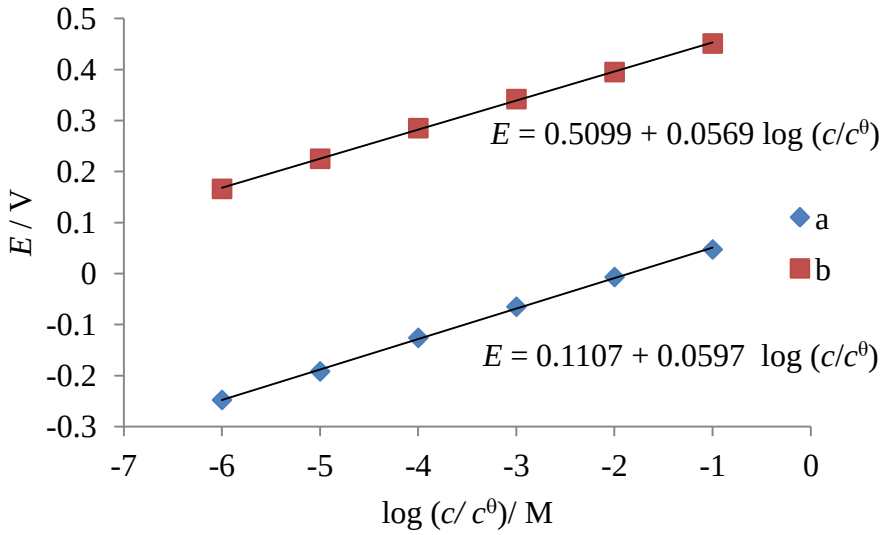

Fig. 16 The response of K^+-ISE against the Ag|AgCl|sat.KCl electrode and the PdH_x electrode. pH value of the aqueous solution: 5.3 ± 0.1.

Conclusions

In the present study, a pH sensor was developed using a modified Pd electrode. The electrode reactions on the surface of the modified Pd electrode were investigated. The modified Pd electrode with PdH_x exhibited good performance in response to the concentration of H^+, based on the redox reaction of the $H_2|H^+$ couple. If the pH value of the aqueous solution is almost constant, the modified Pd electrode can certainly be used as a reference electrode without the risk of release of the inner electrolyte such as KCl. Since the modified Pd electrode can be regenerated by the electrolysis, it is advantageous to serve as the reference electrode for the remote control system or for the environmental observation. In addition, it is useful to measure the accurate evaluation of the concentration of major nutrition components (K^+, Pi, and NO_3^-) in soil because the release of electrolytes (KCl, *etc.*) don't occur.

References

[1] R.W. Sabnis, *Handbook of Acid-Base Indicators*. CRC Press, San Francisco, 2007.

[2] J.A. Pierce, H. Montgomery, A Microquinhydrone Electrode: Its Application to the Determination of the pH of Glomerular Urine of Necturus, J. Biol. Chem. 110 (1935) 228–243.

[3] P.K. Glasoe, F.A. Long, Use of Glass Electrodes to Measure Acidities in Deuterium Oxide1, 2, J. Phys. Chem. 64 (1960) 188–190.

[4] D.D. Macdonald, P.R. Wentrcek, A.C. Scott, Measurement of pH in aqueous systems at elevated temperatures using palladium hydride electrodes, J. Electrochem. Soc. 127 (1980) 1745-1751.

[5] J. Park, J. Kim, H. Quan, A Surface Renewable Iridium Oxide-Glass Composite Hydrogen Ion Electrode, Microchem. J. 95 (2010) 102–106.

[6] U. Oesch, D. Ammann, W. Simon, Ion-Selective Membrane Electrodes for Clinical Use, Clin. Chem. 32 (1986) 1448–1459.

[7] M. Stred'ansky, A. Pizzariello, S. Stred'anská, S. Miertuš, Amperometric pH-Sensing Biosensors for Urea, Penicillin, and Oxalacetate, Anal. Chim. Acta 415 (2000) 151–157.

[8] M. Serrapede, G.L. Pesce, R.J. Ball, G. Denuault, Nanostructured Pd Hydride Microelectrodes: In Situ Monitoring of pH Variations in a Porous Medium, Anal. Chem. 86 (2014) 5758–5765.

[9] L. Qingwen, L. Guoan, S. Youqin, Response of Nanosized Cobalt Oxide Electrodes as pH Sensors, Anal. Chim. Acta 409 (2000) 137–142.

[10] G.K. Mani, M. Morohoshi, Y. Yasoda, S. Yokoyama, H. Kimura, K. Tsuchiya, ZnO-Based Microfluidic pH Sensor: A Versatile Approach for Quick Recognition of Circulating Tumor Cells in Blood, ACS Appl. Mater. Interfaces 9 (2017) 5193–5203.

[11] T. Lindfors, A. Ivaska, pH Sensitivity of Polyaniline and Its Substituted Derivatives, J. Electroanal. Chem. 531 (2002) 43–52.

[12] B. Lakard, D. Magnin, O. Deschaume, G. Vanlancker, K. Glinel, S. Demoustier-Champagne, B. Nysten, P. Bertrand, S. Yunus, A.M. Jonas, Optimization of the Structural Parameters of New Potentiometric pH and Urea Sensors Based on Polyaniline and a Polysaccharide Coupling Layer, Sensors Actuators B. Chem. 166-167 (2012) 794–801.

[13] W.R. Heineman, H.J. Wieck, A.M. Yacynych, Polymer Film Chemically Modified Electrode as a Potentiometric Sensor, Anal. Chem. 52 (1980) 345–346.

[14] I. Toru, W. Kirsty-Jo, D. Guy, Fabrication and Characterization of Nanostructured Pd Hydride pH Microelectrodes, Anal. Chem. 78 (2006) 265-271.

[15] D.K. Nordstrom, C.N. Alpers, C.J. Ptacek, D.W. Blowes, Negative pH and Extremely Acidic Mine Waters from Iron Mountain, California, Environ. Sci. Technol. 34 (2000) 254–258.

[16] L.Y. Beaulieu, K.W. Eberman, R.L. Turner, L.J. Krause, J.R. Dahn, Colossal Reversible Volume Changes in Lithium Alloys, Electrochem. Solid-State Letts. 4 (2001) A137-A140.

[17] J. Watanabe, N. Ikeda, J. Mizutani, N. sato, S. Jin, T. Hirai, H. Ariga, Comparison of Microbiological and Chemical Characteristics among Types of Traditionally Fermented Milk in Inner Mongolia in China ans Calpis Sour Milk, Milk Science 47 (1998) 1-8.

[18] L.M. Okigbo, G.H. Richardson, R.J. Brown, C.A. Ernstrom, Interactions of Calcium, pH, Temperature, and Chymosin During Milk Coagulation, J. Dairy Sci. 68 (1985) 3135-3142.

[19] E. Medina, C. Romero, M. Brenes, A. De Castro, Antimicrobial Activity of Olive Oil, Vinegar, and Various Beverages against Foodborne Pathogens, J. Food Protection 70 (2007) 1194-1199.

[20] N. Nunomura, M. Sasaki, Y. Asao, T. Yokotsuka, Shoyu Volatile Flavor Components: Basic Fraction, Agric. Biol. Chem. 42 (1978) 2123-2128.

[21] D.S. Domingues, H.W. Takahashi, C.A.P. Camara, S.I. Nixdorf, Comput. Electron. Agricul. 84 (2012) 53-61.

[22] A. Reddy, D.F. Noorris, S.S. Momeni, B. Waldo, J.D. Ruby, The pH of beverages in the United States, J. Am. Dent. Assoc. 147 (2016) 255-263.

[23] S. Wongkhantee, V. Patanapiradej, C. Maneenut, D. Tantbirojn, Effect of Acidic Food and Drinks on Surface Hardness of Enamel, Dentine, and Tooth-coloured Filling Materials, J. Dentistry 34 (2006) 214-220.

Chapter 4

Construction of an Automatic Nutrient Solution Management System of Nutrient Solution for Hydroponics

In order to alleviate the world food problem and to realize sustainable agriculture, a reusable and eco-friendly cultivation is urgently required. An automatic management system for nutrient solutions was constructed using a programmable logic controller (PLC) and a K^+-ion selective electrode (K^+-ISE). The concentration of K^+, as a model nutrient, was monitoring by the K+-ISE. When the concentration of K^+ fell to the threshold limit, an appropriate amount of a concentrated K^+ solution was added to the hydroponic solution by use of the PLC. In addition, the volume of the nutrient solution was also maintained at a constant level by automatic addition of water when the current flow between two electrodes ceased owing to exposure of one of the electrodes to air. Since any computers and pumps do not need, the present cultivation system will be constructed simply and inexpensively.

Introduction

An increase in food production is necessary owing to the rapid global population growth in recent years. However, there are difficulties associated with the rapid increase in food production owing to the scarcity of land suitable for agriculture [1-2]. In addition, it is hard to supply food at a constant rate owing to seasonal variations in weather and damage caused by blight, insects, and environmental conditions [3]. Gericke first suggested hydroponics as a means of soil-free agricultural crop production by the use of nutrient solutions [4]. Since then, many people have become interested in the cultivation of fresh vegetables and flowers without soil. Hydroponics has become significantly more widespread in commercial horticulture since Cooper invented the nutrient film technique (NFT), which exploits a flow system comprising a thin nutrient solution layer around the roots of the crop [5-7]. In comparison with conventional soil-based agriculture, hydroponics presents many advantages. For instance, hydroponics does not depend on the features of land nor weather conditions. Furthermore, insect damage and the influence of disease seem to be lessened. Furthermore, it is easy to control the irradiation (period and strength) and temperature during cultivation. Since the nutrients can be reused, the culture media can be utilized without waste [8]. Several research groups have reported that the yields and quality of fruits and vegetables can be improved by optimizing culture conditions [9-11].

Since hydroponic products are usually more expensive than those grown by conventional means owing to the higher running costs, the construction of more efficient systems is demanded. Accordingly, the optimum conditions for the growth of plants have been established [12]. Although changes in the concentrations of nutrient components can been observed by methods such as spectroscopic,

chromatographic, and electrochemical analysis, these are not suitable for real-time monitoring because they require pretreatments such as sampling and filtration [13-14].

It has been established that the electrical conductivity of a hydroponic nutrient solution generally depends on the total concentration of the major nutrient components [15-16]. As for the monitoring of nutrient components using several ion sensors, there are some papers [17-22]. In recent years, several researchers have reported automatic control systems for nutrient components and automated pH and nutrient control systems that rely on conductometry have been developed [23-25]. However, although pH can be successfully controlled to a certain level, the automatic control of various nutrient species (N, P, and K) without any computers and pumps has not been realized until now [26].

In the present study, we designed an automatic nutrient control system for a hydroponic system comprising a programmable logic controller (PLC) and a K^+-ion-selective electrode (K^+-ISE) without any computers and pumps. Here, K^+-ISE was utilized to detect the concentration of K^+ as a typical nutrient. In addition, the volume of the nutrient solution is automatically maintained by a water supply system.

Experimental

Reagents and chemicals

Valinomycin (AG Scientific, Inc., USA), sodium tetraphenylborate (NaTPhB, Kanto Chemical Co., Inc., Japan), potassium chloride (KCl, Wako Co., Ltd., Japan), polyvinyl chloride (PVC, Wako Co., Ltd., Japan), 2-nitrophenyl octylether (NPOE, Dojindo Molecular Technologies Inc., Japan), and tetrahydrofuran (THF, Wako Co., Ltd., Japan) were purchased. All chemicals were reagent grade and were used without further purification.

Apparatus

Electrochemical measurements were conducted using an HE-106A electrometer (Hokuto Denko Co., Ltd., Japan), an HA1010mM1A potentiostat/galvanostat (Hokuto Denko Co., Ltd., Japan), an HB305 function generator (Hokuto Denko Co., Ltd., Japan), and a GL900 A/D converter (Graphtec Co., Ltd., Japan). The pH value of the solution was measured using a PH-230SD pH meter (Lutron Co., Ltd., Taiwan). The automatic management system was constructed using an RS Pro PLC (RS Co., Ltd., UK), an infusion set (NEOfeed, TOP Co., Ltd., Japan), and a power supply unit for illumination (ISC-201-2, CCS Co., Ltd. Japan). A hydroponics device (Green Farm Cube, UING Co., Ltd., Japan) was used to grow vegetable seedlings. In order to check the mechanical function of the automatic nutrient control system, a pump (Unimor UPS-112E, Nitto Kohki, Co., Ltd., Thailand) was used to draw the culture solution.

Fabrication of K^+-ion selective electrodes

Potassium tetraphenylborate (KTPhB) was synthesized by the following steps: First, 10 mL of 0.1 M NaTPhB was mixed with an aqueous solution containing excess KCl, and the mixture was stirred for 2 h. The precipitated KTPhB was isolated by filtration and washed with distilled water. The precipitate was dried at 50 °C under vacuum.

A liquid-membrane type K^+-ISE was prepared as follows. A responsive membrane was prepared by drying a THF solution (1.5 mL) containing 0.04 g of valinomycin, 0.004 g of KTPhB, 0.152 g of PVC, and 0.304 g of o-NPOE. The end of a pipette tip (1 mL) was cut and the cross-sectional area was about 0.1 cm^{-2}. Then, the top was soaked in the THF solution. After vaporization, the PVC membrane was prepared at the end of the pipette tip. Then, 1.5 mL of 0.1 M KCl was placed into the pipette tip and an Ag|AgCl electrode was inserted. The pipette tip was then covered with a rubber stopper. The structure and appearance of the K^+-ISE are shown in Fig. 1. A more detailed construction method is given in the SI. Fig. 2 shows the construction of the measurement system of the K^+-ISE.

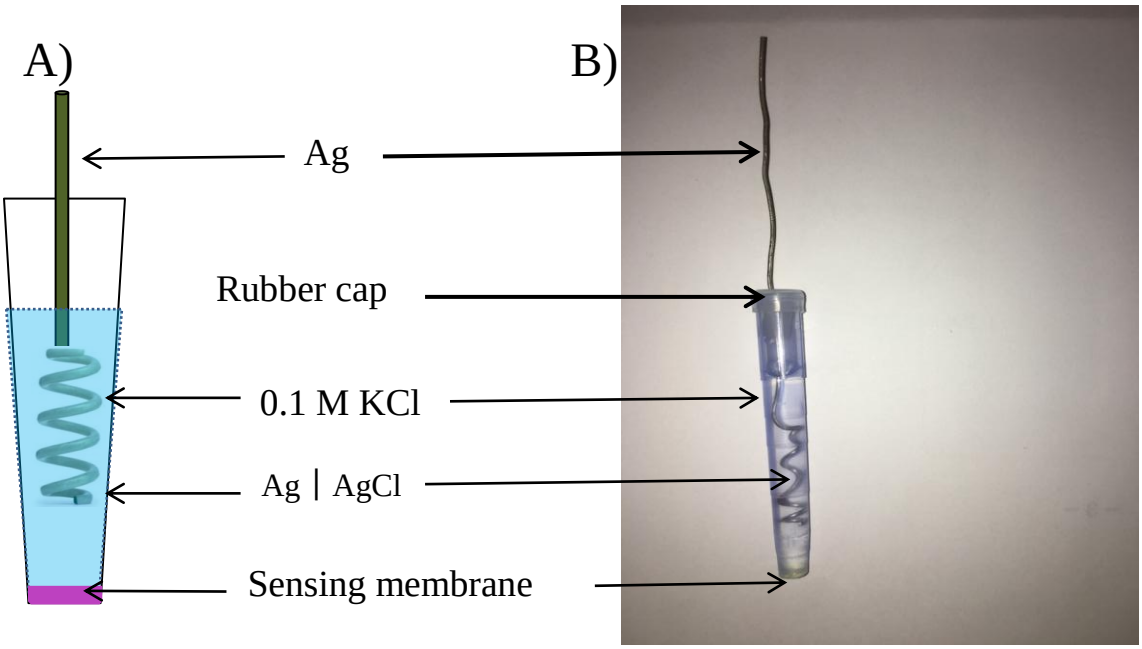

Fig. 1 Design of the K^+-selective electrode (A) and actual appearance of the K^+-ISE (B)

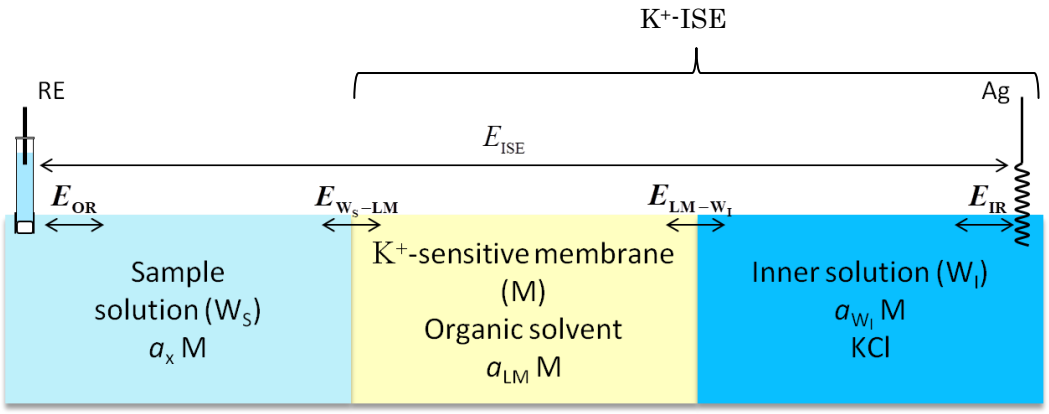

Fig. 2 Principle of liquid membrane ion selective electrode.

Fig. 2 shows the construction of the measurement system of the K^+-ISE.

The potential differences of two aqueous|membrane interfaces are indicated based on Nernst equation. Therefore, the potential difference between the inner aqueous solution (W_I) and the K^+ responding membrane (M) is expressed by eqn. (4-1) and that between M and the sample solution (W_S) is indicated by eqn. (4-2).

$$E_{W_S-LM} = -E^{\circ\prime} + \frac{RT}{F}\ln\frac{a_x}{a_M} \tag{4-1}$$

$$E_{LM-W_I} = E^{\circ\prime} - \frac{RT}{F}\ln\frac{a_{WI}}{a_M} \tag{4-2}$$

Here, $E^{\circ\prime}$ is the standard potential for the transfer of K^+ from W to NPOE, R is the gas constant, T is the thermodynamic temperature, F is the Faraday constant, a_M is the activity of K^+ in M, a_{WI}, is the activity of K^+ in W_I, and a_X is the activity of K^+ in W_S. The potential difference (E_{ISE}) between the K^+-ISE and the reference electrode is represented by eqn. (4-3).

$$E_{ISE} = E_{IR} + E_{OR} + \frac{RT}{F}\ln\frac{a_x}{a_{WI}} = 2.303\frac{RT}{F}\log a_{W_S} + const.$$
$$= 0.0591\log a_{W_S} + const. \tag{4-3}$$

Characteristics of the K^+-ISE

All electrometrical measurements were carried out with a two-electrode system using a reference electrode (Ag|AgCl|sat. KCl) and K^+-ISEs (3 sets). The selectivity coefficient (k_{ij}^{pot}) of the ion j was

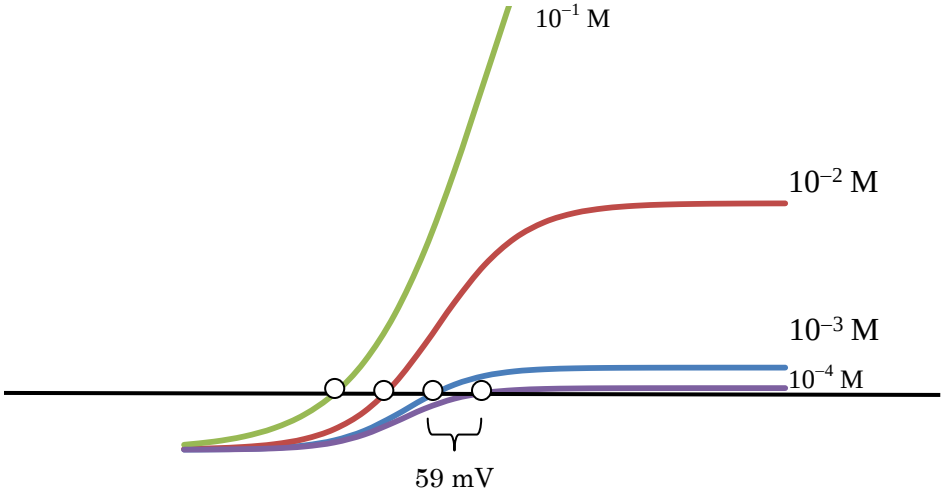

Fig. 3 Schematic voltammograms for the transfer of K^+ at the interface between the K^+-sensitive membrane of the K^+-ISE system and the sample solution when the membrane phase is regarded as the criterion phase.

evaluated against the coexisting ion *j* based on the mixed-solution method. The potential of the K^+-ISE is obtained from Eq. 4-5.

$$E_{ISE} = E_i^{\circ} + \frac{RT}{z_i F} \ln \left(a_i + \sum_{j \neq i} k_{il}^{pot} a_j^{\frac{z_i}{z_j}} \right) \tag{4-5}$$

where $E_i°$ is a constant that depends on the property of the ion *i*, z_i and z_j are the charge numbers of the ions *i* and *j*, *F* is the Faraday constant, a_i and a_j are the activities of the ions *i* and *j*, *R* is the gas constant, and *T* is the temperature. As for E_{ISE}, the interpretation based on the ion transfer voltammetry at the interface between the aqueous and the NPOE solutions is noted using Fig. 3.

Fig. 3 indicates the schematic voltammograms for the transfer of K^+ at the interface between the K^+-sensitive membrane of the K^+-ISE system and the sample solution when the membrane phase is regarded as the criterion phase (the side inserted with the reference electrode). In the potentiometric study, the zero-current potential depends on the concentration of the objective ion in the sample solution. These schematic voltammograms are drawn based on the concept of the voltammetry for the ion transfer at the interface between the aqueous and the organic phase. In the case of the measurement using the K^+-ISE, the potential difference is expressed against the reference electrode in the sample solution. Since the sign of the potential difference is reversed, the zero-current potential of the K^+-ISE (the ISE potential) is shifted in the positive direction as the

concentration of K^+ increases. The ISE potential The K^+-selective electrode displayed a linear response to the concentration of K^+ with a Nernstian slope of –59 mV decade^{-1}, in the K^+ concentration region between 10^{-5} to 10^{-1} mol dm^{-3}. The detection limit was 10^{-6} mol dm^{-3}.

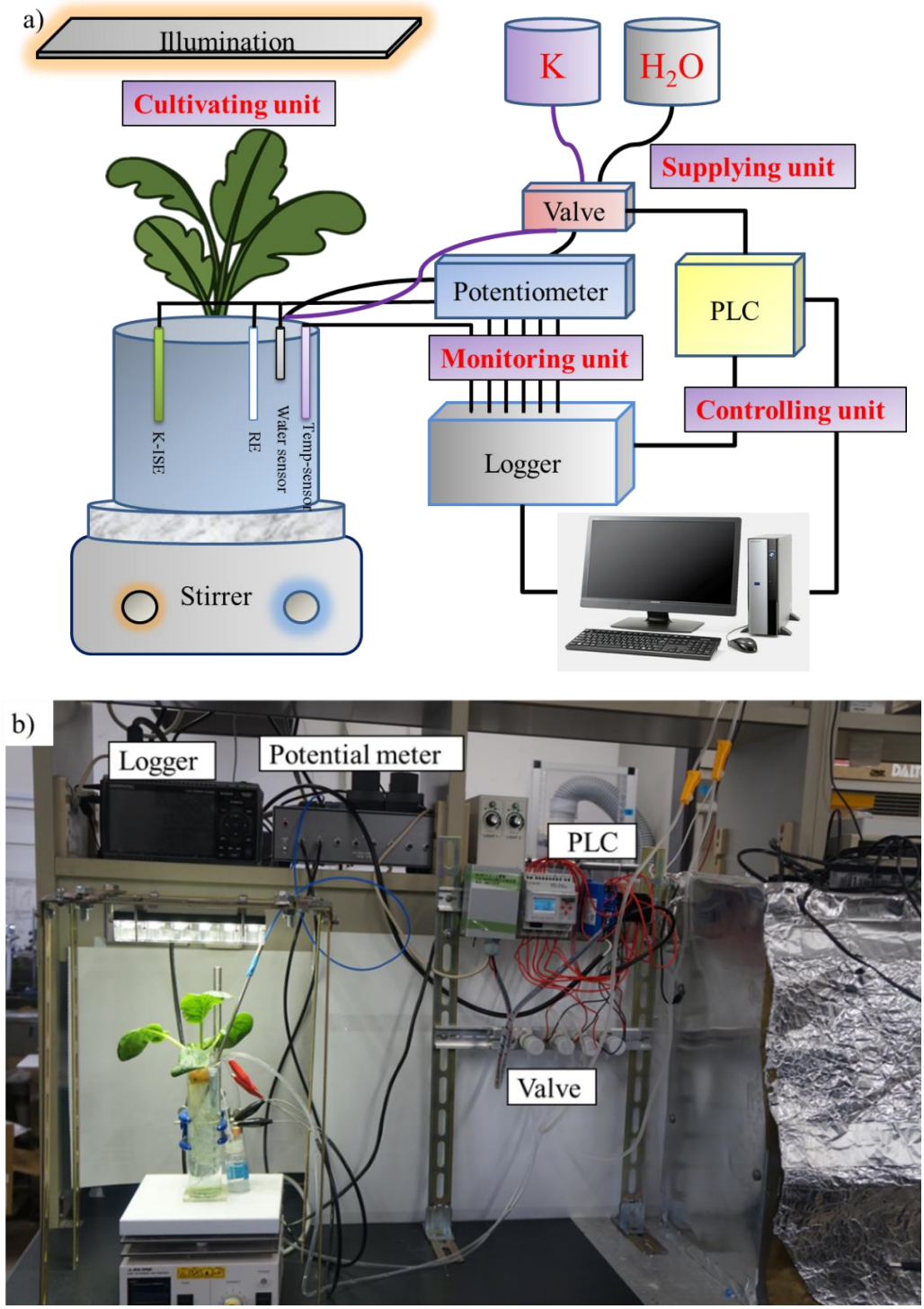

Fig. 4 Design of the automatic management system (a) and its actual appearance (b).

Design of the automatic K^+ concentration management system

As shown in Fig. 4, the automatic management system comprises four units. In the cultivation unit, green plants are cultured in a container filled with a hydroponic solution. A K^+-ISE, a reference electrode, a water volume sensor, and a temperature sensor are placed in the container. The hot-plate stirrer fitted with a thermostat is employed to homogenize the solution. An LED illumination device was set up to allow the growing of green plants.

In the monitoring unit, the potential difference between the K^+-ISE and the reference electrode was recorded in a computer using a potentiometer and a logger. The temperature sensor was directly connected to the logger.

In the control unit, a programmable logic controller (PLC) is connected to the logger and the computer is used just as a recorder. Figure 5 shows PLC software interfaces of the nutrient supply system and the volume control system. When the potential of the K^+-ISE drops beneath a certain level, an alarm from the logger is triggered. The signal reaches the PLC and the valve on the tank of the aqueous solution containing 0.5 M KCl is opened, delivering 1 mL of the solution to the system. Furthermore, a water level sensor made by a Pt wire was used to keep the volume of the nutrient solution constant. When the electric connection between the Pt wire and the reference electrode is broken due to the lowering of the water level, an alarm is triggered, similarly to the K^+-ISE system. When this alarm is activated, 5 mL of water is added to the solution.

Fig. 5 (A) shows the operation interface of the nutrient management system. Here, I means a digital input for the base module. T (or t) means a timer function which can be used in different modes. Q (or q) means an output point of potential free for the base module, and a delay time can be set by this function. Capital letters (I, T, and Q) indicate the points switched on, and small letters (t and q) are the points switched off. The analog input for the base module used in the analog function. The inputs signal garneted from the alarm of the logger. Trigger and reset are input into all timers. The open time and the close time can be set by this function. Fig. 3 (B) indicates the operation interface of the volume keeping system. The flow chart is written below, and the water volume and the concentration of K^+ were controlled.

In the supplying unit, the programmable logic controller was connected to the valve to supply 1 mL of the K^+ solution, and the other valve was opened just after the signal was received. Similarly, 5 mL of water was added in the case of receiving the alarm due to the decrease of the volume of the nutrient solution.

Thus, the concentration of K^+ in the nutrient solution is monitored during cultivation, and the volume of the nutrient solution is kept at an almost constant level.

A)

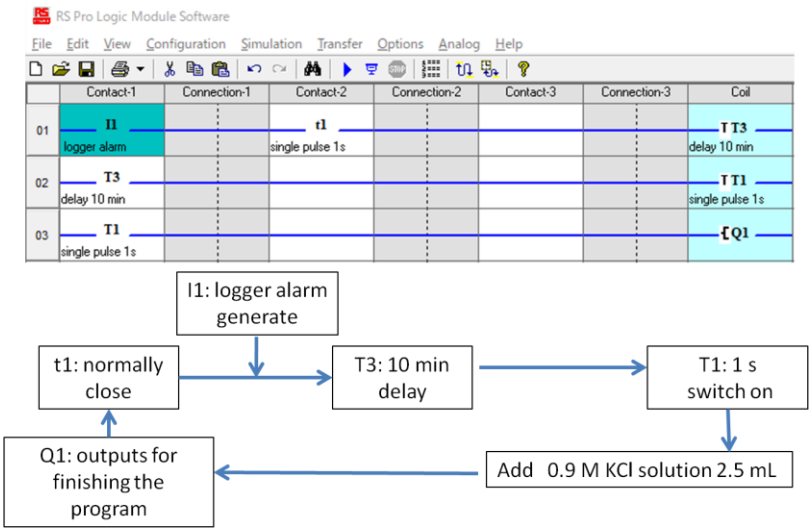

B)

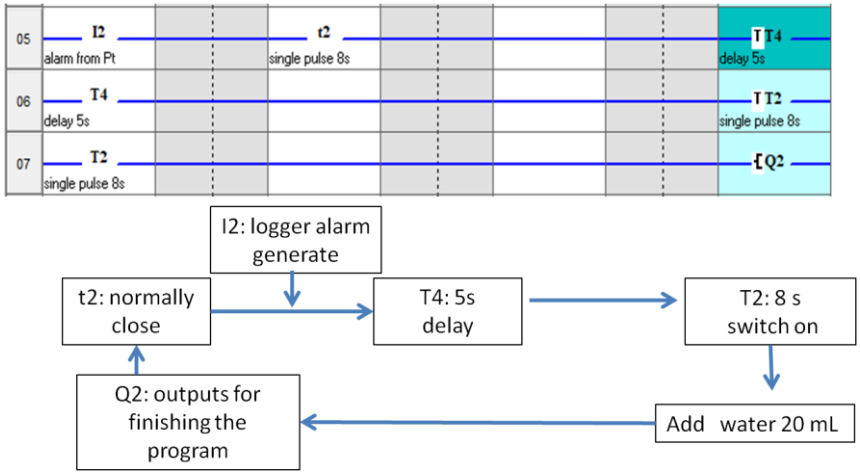

Fig. 5 Software interface of the programmable logic controller of nutrient supply system (A) and volume control system (B).

Operation checking for the automatic supply system

Only to prove that the water supply system works according to the break in the electric connection between the nutrient solution and a platinum wire electrode, a pump (Unimor UPS-112E, Nitto Kohki, Co., Ltd., Thailand) was used. For performance checking, water was injected into the cultivation device by the pump at a flow speed of 100 mL min^{-1}. At the same time, the nutrient solution was flushed from the cultivation device at the same flow speed. The nutrient solution was artificially diluted until the concentration falls below the threshold (0.001 M), at which point 1 mL of 0.55 M K^+ nutrient solution is added. In this way, the K^+-concentration of the nutrient solution was kept at a largely constant value. This time, 0.55 M K^+ was added to easily recognize the control system. Therefore, it is appropriate to add the diluted solution (e.g. 0.01 M) to the culture solution.

Practical plant cultivation using the control system

Brassica rapa was cultivated in a commercial hydroponic nutrient solution for 20 days. The water level was controlled by the water volume sensor. The threshold of the potential was set at –0.028 mV, which corresponded to 0.005 M. The concentration of the additive KCl solution was 0.5 M, and the volume of every addition was 1 mL.

Results and Discussion

Response characteristics of the K^+-ISE

The K^+-ISE shows a linear response to K^+ in the concentration range 10^{-6}–10^{-1} M with a slope of −59.7 mV dec^{-1}, as shown in Fig. 6. The practical response time was recorded by changing the concentration of K^+ from 1×10^{-6} M to 1 M, as shown in Fig. 6 inset. The potential reaches a constant value within 5 s of the addition of KCl into the cell system. The fluctuation of the potential at the same concentration is within ±2 mV over 24 h. The potential response of the K^+-selective electrode is very stable, as previously reported by several research groups.[27-28] The selectivity coefficient (k_{ij}^{pot}) is usually given by Eq. 1. As shown in Table 1, the K^+-ISE exhibits excellent selectivity in the presence of other common cations. Thus, it was successfully utilized as a potassium sensor in the present automatic management system.

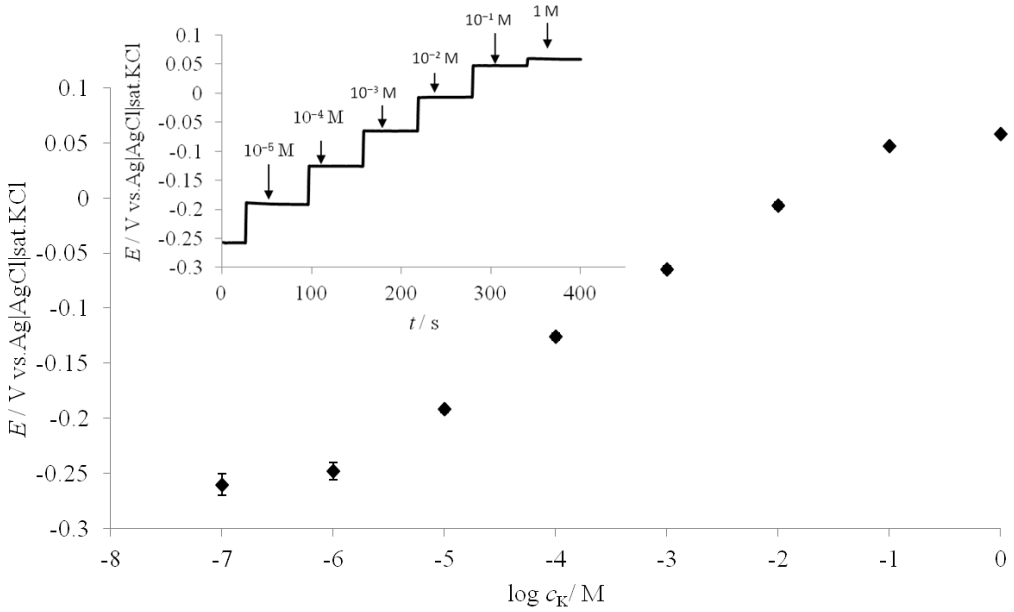

Fig. 6. Calibration plot of the K^+-ISE, and response time curve of the K^+-ISE (Inset).

Table 1 Selectivity coefficients of common cations

Anion	log (k_{ij}^{pot})
Na^+	−5.5 ± 0.2
Mg^{2+}	−4.0 ± 0.3
Ca^{2+}	−5.0 ± 0.3
NH_4^+	−3.1 ± 0.2

Monitoring of the K+ concentration during the plant cultivation and volume control of the nutrient solution

Figure 7（a） shows the time-course of the potential change for the K^+-ISE during plant cultivation. Arrows indicate the points at which water was automatically supplied by the water volume control system. Thus, the water volume is maintained around a certain level throughout plant cultivation. In addition, it was confirmed that the K^+ is exhausted by *Brassica rapa* after two weeks.

As shown in Fig. 7(b), the potential value is maintained in the region between –0.040 and 0.005 V, and the fluctuation is within ±3 mV. It can be verified that the automatic control system maintains the concentration of the nutrient component within the 0.005–0.02 M range. If the amount of KCl added is decreased, this concentration region can be narrowed. In the present case, these conditions were selected to more clearly assess the management of nutrient control.

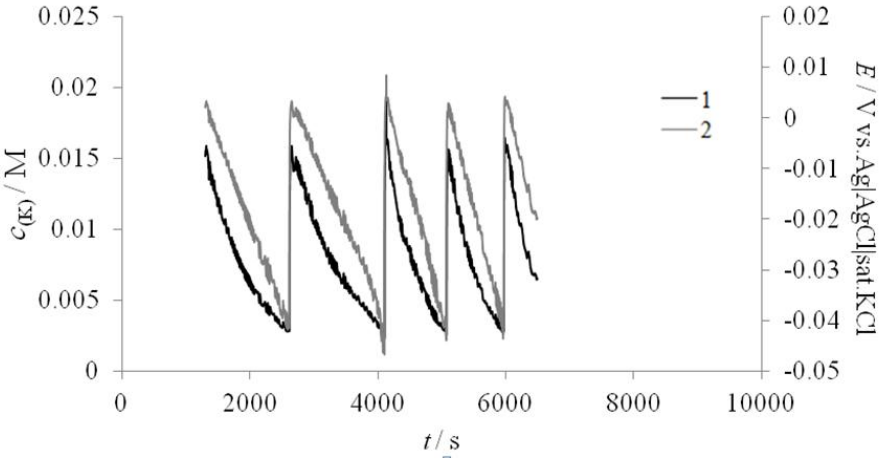

Fig. 7. Monitoring of the concentration of K^+ during the plant cultivation (a) and potential change of the K^+-ISE under the simulation condition (b); Arrows indicate the points at which water (A) or 0.5 M KCl (B) is supplied. 1: concentration of K^+; 2: potential of the K^+-ISE.

Construction of the automatic nutrient solution management system

By combining the concentrated KCl solution supply system and the water supply system, an automatic nutrient management system was constructed. As indicated in Fig. 8, the concentration of K^+ is controlled within a fixed value (0.0055 ± 0.0010 M). If the amount of KCl added is decreased, the concentration of K^+ can be controlled around the threshold value more precisely.

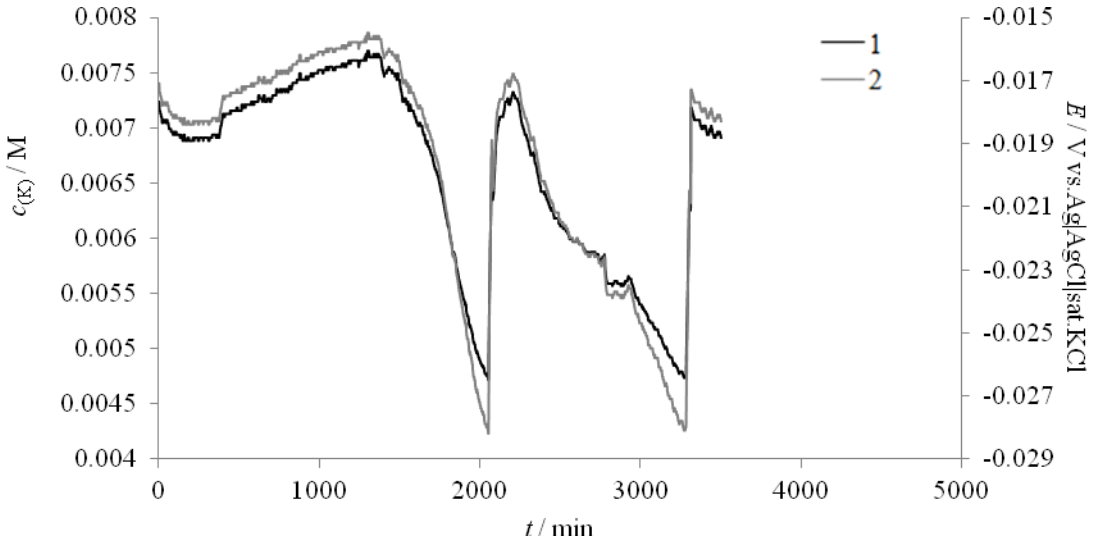

Fig. 8. Practical testing of the automatic management system. 1: Concentration of K^+ in the cell system; 2: Potential of the K^+-ISE.

Conclusion

As a step toward realizing artificially intelligent plant factories, an automatic management system for water volume and nutrient concentration without computer-control or pumps was constructed. Comparing with the conventional automatic systems, the present system was much more simple and inexpensive. This is the first report of an automatic management system for both the volume of the nutrient solution and its concentration. Although the present equipment is very simple, the volume of the nutrient solution and the concentration of the objective nutrient component (K^+) were kept almost constant during plant cultivation. This makes precise control of the eco-friendly hydroponic system possible. In the future, several nutrient components in the hydroponic nutrient solution (potassium, phosphate, and nitrite) will be controlled simultaneously. In addition, pH, temperature, humidity, and illumination should be added to the automatic management system.

References

[1] D. Despommier, The rise of vertical farms, Sci. Am. 301 (2009) 80–87.

[2] M.D. Sardare, S. V Admane, A review on plant without soil-hydroponics, Int. J. Res. Eng. Technol. 2 (2013) 299–304.

[3] T. Coolong, Hydroponic lettuce, Univeristy Kentucky Coop. Sxtention Serv. (2012) 1–4.

[4] Gericke, W. F., HYDROPONICS--CROP PRODUCTION IN LIQUID CULTURE MEDIA, Science, 85 177-178.

[5] A. Cooper, others, The ABC of NFT. Nutrient film technique., Grower Books., 1979.

[6] W.W. Leonhardt, K.W. and McCall, Hydroponics, Hawaii Cooperative Extension Service, Hawaii, 1914.

[7] H.M. Resh, Hydroponic Food Production, Crc Press. (2012).

[8] D. Savvas, K. Adamidis, Automated management of nutrient solutions based on target electrical conductivity, pH, and nutrient concentration ratios, J. Plant Nutr. 22 (1999) 1415–1432.

[9] M. Rodriguez Santamaria, V.J. Flórez, others, Changes in ec, ph and in the concentrations of nitrate, ammonium, sodium and chlorine in the drainage solution of a crop of roses on substrates with drainage recycling, Agron. Colomb. Vol. 30, Núm. 2 (2012); 266-273 Agron. Colomb. Vol. 30, Núm. 2 (2012); 266-273 2357-3732 0120-9965. (n.d.).

[10] P.G. Pardey, J.M. Alston, V.W. Ruttan, The economics of innovation and technical change in agriculture, in: Handb. Econ. Innov., Elsevier, 2010: pp. 939–984.

[11] A.J. Cooper, Crop production in recirculating nutrient solution, Sci. Hortic. (Amsterdam). 3 (1975) 251–258.

[12] F. Benoit, N. Ceustermans, Consequences of closed soilless growing systems for the recirculating nutrient solution and the production techniques, Acta Hortic. 633 (2004) 331–340.

[13] B. Bernstein, Class and pedagogies: Visible and invisible, Educ. Stud. 1 (1975) 23–41.

[14] M. Jensen, H. 1999. Hydroponics Worldwide, Acta Hortic. 481 (n.d.) 719–730.

[15] T.C. Paulitz, R.R. Bélanger, Biological control in greenhouse systems, Annu. Rev. Phytopathol. 39 (2001) 103–133.

[16] G.L. Barbosa, F.D.A. Gadelha, N. Kublik, A. Proctor, L. Reichelm, E. Weissinger, G.M. Wohlleb, R.U. Halden, Comparison of land, water, and energy requirements of lettuce grown using hydroponic vs. conventional agricultural methods, Int. J. Environ. Res. Public Health. 12 (2015) 6879–6891.

[17] W.J. Albery, B.G.D. Haggett, L.R. Svanberg, The development of sensors for hydroponics, Biosensors, 1 369-397.

[18] N.G. Osmolovskaya, V.A. Novak, L.N. Kuchaeva, V.V. Kurilenko, K.N. Mikhelson, Portable Ion Selective Technique in Field Screening of Plants Pollution, 1997.

[19] H.J. Kim, W.-K. Kim, M.-Y. Roh, C.-I. Kang, J.-M. Park, K.A. Sudduth, Automated sensing of hydroponic macronutrients using a computer-controlled system with an array of ion-selective electrodes, Computers & Electronics in Agriculture, 93(2013)46-54.

[20] G. Vardar, M. Altıkatoğlu, D. Onat, M. Cemek, I. Işıldak, Measuring calcium, potassium, and nitrate in plant nutrient solutions using ion-selective electrodes in hydroponic greenhouse of some vegetables, Biotechnology & Applied Biochemistry, 62 (2014) 663-668.

[21] H.J. Kim, D.-W. Kim, W.K. Kim, W.-J. Cho, C.I. Kang, PVC membrane-based portable ion analyzer for hydroponic and water monitoring, Computers & Electronics in Agriculture, 140(2017)374-385.

[22] W.J. Cho, H.J. Kim, D.H. Jung, D.W. Kim, J.E. Son, On-site ion monitoring system for precision hydroponic nutrient management, Computers & Electronics in Agriculture, 146 (2018) 51-58.

[23] D.-H. Park, B.-J. Kang, K.-R. Cho, C.-S. Shin, S.-E. Cho, J.-W. Park, W.-M. Yang, A study on greenhouse automatic control system based on wireless sensor network, Wirel. Pers. Commun. 56

(2011) 117–130.

[24] D.S. Domingues, H.W. Takahashi, C.A.P. Camara, S.L. Nixdorf, Automated system developed to control pH and concentration of nutrient solution evaluated in hydroponic lettuce production, Comput. Electron. Agric. 84 (2012) 53–61.

[25] V. Palande, A. Zaheer, K. George, Fully Automated Hydroponic System for Indoor Plant Growth, Procedia Comput. Sci. 129 (2018) 482–488.

[26] M.A. Saad, H.M. Abdelsamei, E.M.A. Ibrahim, A.M. Abdou, S.A. El Sohaimy, Effect of pH, heat treatments and proteinase K enzyme on the activity of Lactobacillus acidophilus bacteriocin, Benha Vet. Med. J. 28 (2015) 210–215.

[27] P.C. Hauser, D.W.L. Chiang, G.A. Wright, A potassium-ion selective electrode with valinomycin based poly (vinyl chloride) membrane and a poly (vinyl ferrocene) solid contact, Anal. Chim. Acta. 302 (1995) 241–248.

[28] J. Pick, K. Toth, E. Pungor, M. Vasak, W. Simson, A potassium-selective silicone-rubber membrane electrode based on a neutral carrier, Anal. Chim. Acta. 64 (1973) 477–480.

Conclusion

In this study, the author constructed two kinds of phosphate ion sensors and a kind of pH sensor. A multi-ion stat was also designed to control the concentration of nutrient solution at a constant level in hydroponic culture.

In chapter 1, phosphate ion-selective electrode was constructed by a Co electrode with cobalt coating phosphate. This electrode exhibited favorable potentiometric responses for the determination the concentration of $H_2PO_4^-$ ion. The sensing mechanism was also investigated in detail.

In chapter 2, the modified-molybdenum electrode as a HPO_4^{2-}-ion selective electrode was explained. The electrode showed a good performance responding to the logarithm of the concentration of (HPO_4^{2-}). The electrode showed acceptable selectivity against common anions such as SO_4^{2-}, NO_3^-, Cl^-, etc. The responding mechanism can be explained by considering both the formation of molybdophosphate complexes and the absorption of $PMo_{12}O_{40}^{3-}$ on the electrode surface.

In chapter 3, a pH sensor was constructed using a Pd electrode. The electrode reactions on the surface of the Pd electrode storing with H_2 gas were investigated. The modified Pd electrode with PdH_x exhibited good performance in response to the concentration of H^+ based on the redox reaction of the $H_2|H^+$ couple. If the pH value of the aqueous solution is almost constant, the modified Pd electrode can certainly be used as a reference electrode without the risk of release of the inner electrolyte such as KCl. Since the modified Pd electrode can be regenerated by the electrolysis, it is advantageous to serve as the reference electrode for the remote control system or for the environmental observation. In addition, it is useful to measure the accurate evaluation of the ion concentration in soil in a minute region because the releases of electrolytes (KCl, etc.) don't occur.

In chapter4, as a step toward realizing artificially intelligent plant factories, an automatic management system for water volume and nutrient concentration without any computer-control or pumps was constructed. Comparing with the conventional automatic systems, the present system was much more simple and inexpensive. This is the first report of an automatic management system for both the volume of the nutrient solution and its concentration. This makes precise control of the eco-friendly hydroponic system possible. In the future, the control system of other conditions such as pH, temperature, humidity, and illumination should be added to the automatic management system.

Acknowledgement

The author wishes to express his sincere gratitude to Dr. Kenji Kano, Professor of Kyoto University for providing him with his kind guidance, valuable discussion, constructive comments and continuous encouragement throughout this study, and Dr. Osamu Shirai, Associate Professor of Kyoto University, for a number of helpful suggestions and criticisms. The author would like to thank Dr. Yuki Kitazumi, Assistant Professor of Kyoto University, for his kind supports and a number of critical comments.

The authors thank Dr. A. Uehara , Associate Prof. K. Mori and Prof. Takayuki Sasaki for help of the measurement of XRD analysis. This work was supported by the donation from Mr. Nobuo Takeshige. This study was supported by The 27th Botanical Research Grant of Ichimura Foundation for New Technology.

The author shows his appreciation to Dr. Keiko Kita, Professor of Kyoto University, Dr. Tatsuo Kurihara, Professor of Kyoto University, Dr. Hisashi Miyagawa, Dr. Naoki Mori, Professor of Kyoto University, Dr. Yasuyoshi Sakai, Professor of Kyoto University, Dr. Kazumitsu Ueda, Professor of Kyoto University, Dr. Mitsuyoshi Ueda, Professor of Kyoto University, Dr. Toshiaki Umezawa, Professor of Kyoto University, and Dr. Takashi Watanabe, Professor of Kyoto University for their critical comments and kind supports.

The author gratefully thanks to the members of Kano's laboratory, Mr. Katsumi Hamamoto, Dr. Yu Sugimoto, Dr. Keisei So, Dr. Hong-qi Xia, Dr. Kento Sakai, Dr. Hibino Yuya, Mr. Yutaka Takeuchi, Mr. Ryutaro Katsube, Mr. Ryosuke Nakamura, Mr. Takuya Yamaguchi, Ms. Yuko Fukao, Ms. Yukina Matsui, Mr. Eisaku Nakao, Ms. Saeko Shiraiwa, Ms. Maiko Kaji, Ms. Akiho Kojima, Ms. Yui Takahashi, Mr. Masaki Takaishi, Mr. Harunori Kawai, Mr. Yuya Kaida, Ms Mizue Wanibuchi, Mr. Taiki Adachi, Mr. Issei Kasai, Ms. Kyoko Kishida, Dr. Dyah Iswantini, Mr. Tastuya Aguro, Mr. Ryouta Arakawa, Mr. Kento Zushi, Mr. Masahiro Miyata, Mr. Yohei Suzuki, Mr. Tetsu Naruse, Mr. Yusuke Yamata, Mr. tatsushi Yoshikawa and Ms.Toshie Koyama, for their kind support in the author's laboratory life.

The author thanks professors, doctors, and friends, the author have ever met in conferences and events for their kind advices and encouragement.

Finally, the author would like to express his greatest thanks to his family for their continuous encouragement.

Xu Kebin

Kyoto

March 2020

List of Publications

1) Xu, K., Kitazumi, Y., Kano, K., and Shirai, O.
Phosphate Ion Sensor Using a Cobalt Phosphate Coated Cobalt Electrode
Electrochimica Acta, **282**, 242-246, (2018). (Chapter 1)
2) Xu, K., Kitazumi, Y., Kano, K., and Shirai, O.
Construction of an Automatic Nutrient Solution Management System for Hydroponics-Adjustment of the K^+-Concentration and Volume of Water
Analytical Sciences, **35**(5), 595-597, (2019). (Chapter 4)
3) Xu, K., Kitazumi, Y., Kano, K., and Shirai, O.
Electrochemical pH Sensor Based on a Hydrogen-storage Palladium Electrode with Teflon Covering to Increase Stability
Electrochemistry Communication, **101**, 73-77 (2019). (Chapter 2)
4) Xu, K., Kitazumi, Y., Kano, K., and Shirai, O.
Design of a Phosphate Ion Selective Electrode Based on Modified Molybdenum Metal
Analytical Sciences, in press. (Chapter 3)